International Climate News

M. J. Arteaga-Garavito R. Colacito M. M. Croce B. Yang*

Abstract

We develop novel high-frequency indices that measure climate attention, covering a wide range of both developed and emerging economies. This is achieved by analyzing the text of over 23 million tweets published by leading national newspapers on Twitter during the period from 2014 to 2022. Our findings reveal that a country experiencing more severe climate news shocks tends to see both an inflow of capital and an appreciation of its currency. In addition, brown stocks experience large and persistent negative returns after a global climate news shock if located in highly-exposed countries. These outcomes align with the predictions of a risk-sharing model in which investors price climate news shocks and trade consumption and investment goods in global markets.

First Draft: June 28, 2023. This Draft: March 15, 2025.
Keywords: International Climate Indices, Text Analysis, Trade, Currencies.
JEL Classification: F3, F4, G1.

*Maria Jose Arteaga-Garavito is a PhD Student at Bocconi University (email: majo_arteaga@hotmail.com; Twitter: @MajoArteaga). Riccardo Colacito is affiliated with the Kenan-Flagler Business School at UNC Chapel Hill and NBER (email: ric@unc.edu; Twitter: @RColacito). Mariano Massimiliano Croce is affiliated with Bocconi University, CEPR, IGIER and Baffi-Carefin (email: mmc287@gmail.com; Twitter: @MCroce_MacroFin); Biao Yang is affiliated to the Shanghai Jiao Tong University (biao.yang@sjtu.edu.cn; Twitter: @Biao90). We thank Elena Carletti, Lars Hasen, Monika Piazzasi and Marcin Kacperczyk for useful feedback on the paper, as well as our discussant Juri Marcucci and Zhe Geng. We also thank seminar participants at the LUISS Finance conference, the SED, the Econometrics Society Meetings (Asia), the CFRN Young Finance Scholars Meeting, the Workshop on AI in Finance and Digital Economy at HKUST (Guangzhou), Shanghai Jiao Tong University, and Peking University.

1 Introduction

In recent years, there has been a growing focus on the interaction between climate dynamics and economic activities. Predicted changes in climate patterns are expected to result in a significant redistribution of economic operations across various locations, sectors, and corporations. At the same time, the valuation of stocks and bonds is increasingly reflecting climate risk factors. However, to the best of our knowledge, there has been limited attention given to the relationship between climate-related news shocks and international economic variables, such as currencies and global capital flows.

In this paper we construct a new index that captures high-frequency climate attention based on the content of the Twitter feeds of major newspapers in both advanced and emerging economies. We document two main findings. First, countries with greater exposure to climate news shocks experience a persistent currency appreciation and a decrease in net exports, highlighting the significant impact of climate news on economic variables. Second, brown firms located in highly exposed countries tend to experience large negative and persistent stock returns after adverse climate news shocks. To the best of our knowledge, we are the first to document no significant effect on high-emission firms located in countries with low exposure to climate news shocks.

Specifically, we employ textual analysis techniques to analyze news articles from major national newspapers posted on Twitter during the period of 2014–2022. In order to form hypotheses on the response of currencies, we start with a flexible no-arbitrage model with complete markets in which (i) climate news shocks are priced, and (ii) countries feature heterogeneous exposure to global climate news shocks. This setting suggests that countries with high exposure to climate news shocks should ex-

perience an appreciation of their currency upon the arrival of adverse global news shocks. When testing this hypothesis using the high-frequency dataset that we constructed, we found evidence that corroborates our prediction. This result adds empirical support to the theoretical link between climate news shocks and currency values.

Additionally, in line with the empirical asset pricing literature, we estimate sensitivity coefficients of returns over various horizons and for more than 17,000 firms. We examine firms with varying emission intensities located in all the countries included in our study. Importantly, in our empirical investigation we use an interaction term comprising emissions and country-level exposure. The literature has already documented that climate attention shocks are followed by negative cumulative stock returns. We find that this effect is highly persistent and is concentrated among brown firms that are located in countries with high exposure. In contrast, brown firms in countries with low exposure exhibit no significant response in their equity returns.

In a second step, we consider a general equilibrium model in which: (i) investors price climate news shocks; (ii) investment goods can be used to increase either green or brown assets; and (iii) there are both productivity and global climate news shocks. This model predicts that a country subject to a relatively more adverse climate news shock should experience both an appreciation of its currency (as in the no-arbitrage model) and a decline in its net exports. Our newly developed indicators can be aggregated at a quarterly level, enabling us to merge our news-based data with international trade data. Our results provide empirical validation for our hypotheses.

In what follows, we provide a more detailed description of the novel contribution related to our climate news index. More specifically, as in Engle et al. (2020), we construct a climate attention index that measures the extent to which climate change is discussed in the news media. However, our method differs in that we focus on news-

papers with a significant presence on Twitter across many countries. This approach allows us to compile a large dataset of over 23 million tweets, which we then aggregate at the country level across daily, weekly, monthly, and quarterly frequencies. We compare the aggregated text to a corpus of authoritative texts on climate change, similar to the method used by Engle et al. (2020). As of the date of this draft, our data coverage refers to a total of 25 countries that span a wide range of local languages, income levels, and geographical regions.

We construct climate news indices at the country level and aggregate them to create a global index by computing cross-country averages weighted equally, by GDP, and by Twitter volume (data available on our website). For each country in our dataset, we regress its country-specific climate index on the global index. The estimated slope, denoted as β, measures each country's exposure to common or, equivalently, global news. Across countries, we find a substantial degree of variation in exposure.

To further assess our text-based indices, we assess the correlation between our estimated β values and alternative measures of climate exposure. We first use the vulnerability score provided by the Notre Dame Global Adaptation Initiative. This comprehensive index aims to encapsulate "a country's exposure, sensitivity, and capacity to adapt to the negative effects of climate change." We observe a positive and statistically significant correlation between our β estimates and this index, implying that countries with higher β values exhibit greater susceptibility to climate change.

In addition, we also consider absolute latitude as a second indicator of climate exposure. Countries situated in regions with lower absolute latitudes are usually considered more exposed to rising temperatures resulting from climate change. We find a negative correlation between our β estimates and absolute latitude, reinforcing the effectiveness of our approach in capturing a country's exposure to climate change.

Importantly, we show that our measure is correlated with vulnerability but not fully subsumed by it, indicating that our exposure coefficients provide additional information beyond what is captured by vulnerability.

Leveraging our granular dataset, we use high-frequency data to identify the impact of climate news shocks on asset prices. Specifically, we analyze the reaction of currencies and stocks in the days following a substantial increase in climate attention. To achieve this, we compute daily innovations in our global climate index and focus on the top 15% of these observations. This approach allows us to (i) reduce noise from non-climate-related news and (ii) better isolate days driven by "pure" climate news shocks. Such a methodology is commonly employed in the literature on identifying the effects of news related to policy announcements (Leombroni et al. 2021). Importantly, some days with substantial climate-related news might fall below the top 15% threshold due to the prominence of other topics in the news. Consequently, as is typical in this literature, we may have a downward bias, i.e., a reduced likelihood of detecting a significant effect of climate news on asset prices and currencies.

We further incorporate a sentiment analysis of climate-related tweets on days with high climate attention. Using the BERTopic algorithm, we cluster all tweets into topics and identify those closely related to climate. This subset is then divided into two groups based on whether the topic primarily pertains to climate-related physical or transition risk. Following this classification, each tweet on a given day is categorized as related to physical risk, transition risk, or non-climate topics. We apply multilingual sentiment classifiers to distinguish between positive and negative content. Our findings indicate that days with extremely high climate attention are predominantly characterized by negative climate-related news. The reaction of currencies and stock returns is mainly driven by negative news about transition risk.

Our analysis using daily-frequency data reveals that currencies of countries with higher exposure to our global climate index tend to appreciate following climate news shocks, with this effect persisting over several days. Remarkably, this finding is observed not only in pairs of advanced economies but also in combinations involving at least one developing country. Moreover, the robustness of this finding is upheld regardless of (i) the method used for aggregating country-level climate indices into a single global index, and (ii) whether we use weekly or daily data.

In the second part of the paper, we develop a general equilibrium model that incorporates a recursive risk-sharing mechanism for both productivity and climate news shocks. To the best of our knowledge, this is the first general equilibrium model in the climate finance literature to incorporate priced climate news and multiple countries. While the model is necessarily stylized to focus on the key mechanism, it provides a novel and valuable framework for understanding the role of this type of risks in an international context. The significance of climate news shocks lies in their impact on the distribution of climate-related utility damages among countries, which are characterized by heterogeneous degrees of exposure to a shared climate news shock. Within this framework, our model demonstrates that when agents price negatively climate news shocks, two outcomes occur in response to an adverse global news shock: the currency of the most exposed country appreciates, and there is a decrease in its net exports, signifying a resource outflow from the least exposed country. We proceed to empirically test these theoretical outcomes using our data set.

We test the predictions of our model by using quarterly trade data combined with our climate index aggregated at the same frequency. As in the model, we find that countries more exposed to climate news shocks tend to become net recipients of capital following adverse climate news, as evidenced by a decrease in their net exports.

Related literature. An important strand of recent literature employs textual analysis of earnings conference call transcripts to assess exposure to climate risk (see, for example, Sautner et al. 2023, Hassan et al. 2019 and Hassan et al. 2023). We differ from this literature in that we focus on the public interest for climate, rather than on educated firm-level experts. Moreover, our access to social media outlets allows us to construct a high-frequency index for a large cross-section of countries.

Our frictionless model builds on the tradition of international macro-finance models with recursive preferences and news shocks (Colacito et al. 2018). We present a unified framework to document that currencies, international capital flows, and investments in brown and green technologies are related to our climate-related news. We leave the study of settings with segmented markets (see, among others, Sandulescu et al. 2020) to future work.

A substantial body of literature has examined the behavior, predictability, and volatility of exchange rates (Della Corte et al. 2009; Della Corte et al. 2011; Della Corte et al. 2016). Our analysis contributes to this stream by focusing on the dynamic response of the foreign exchange market to news. In international asset pricing, extensive research has developed and analyzed models to understand asset prices, exchange rates, and macroeconomic interactions across countries (Pavlova and Rigobon 2007, 2010, 2013; Hassan 2013; Hassan et al. 2015, 2016; Zviadadze 2017). We contribute to the broader understanding of international macroeconomic dynamics and asset valuation in response to global climate-related events.

Another line of research investigates the impact of political and economic risk on firms, asset markets, and international economic linkages (Hassan et al. 2019, 2023). This literature develops methodologies to quantify various risks and uncertainties and assesses their economic and financial spillovers. Our study introduces a novel

text-based measure of global attention to climate change as an indicator of perceived risk and uncertainty. Furthermore, we document the influence of our index on currency markets and international financial dynamics.

The literature on carry trade strategies has linked their risk premia to global risk factors (see, for example, Lustig et al. 2011, 2014; Mueller et al. 2017). Our results suggest that climate-related global news is an important risk factor for both exchange rate movements and capital flows.

Lee et al. (2022) find heterogeneous impulse responses of monthly U.S. dollar (USD) real exchange rates of 76 countries to global temperature shocks. We differ from their work in several dimensions: (i) we have a broader cross-section of country pairs; (ii) our climate-related indices move with a broad set of climate-related news, not just realized temperature changes; and (iii) we link both currencies and international current accounts. Javadi et al. (2023) find no link between G10 currencies and the vulnerability of these countries to physical climate risk. Our broader indicator captures both physical and transition risk and suggests the presence of a relevant link at both the daily and the weekly frequency.

Our work is related to the evolving academic field of climate finance (see, among others, Giglio et al. 2021a, b, 2023; Starks 2023; Hsu et al. 2023; Bansal et al. 2019; Pástor et al. 2021, 2022; Colacito et al. 2019; Acharya et al. 2022; Bolton and Kacperczyk 2023, 2021; Bolton et al. 2023; and Kashyap et al. 2024). The climate macro-finance literature has primarily focused on the link between climate risks, local assets and local macroeconomic dynamics. We differ from these studies for our attention to international quantities and currencies.

2 Data

Data collection. In line with the methodology developed in Engle et al. (2020), we construct a climate attention index to assess the extent of discourse concerning climate change within the news media. Our approach differs from that of Engle et al. (2020) in that we have chosen to focus on news media outlets, particularly newspapers, that have a strong presence on the social media platform Twitter.[1] Utilizing textual analysis, we generate country-level indices at both low and high frequencies. As of the date of this draft, our dataset encompasses a total of 25 countries, providing a comprehensive representation across a wide spectrum of local languages, income levels, and geographical regions. We have conveniently summarized our dataset in Table 1.

Climate attention index construction. We use the "universe" of Tweets from October 2014 until December 2022 from the Twitter accounts of official newspapers (the full list of newspapers is reported in table A.1 in the appendix). We construct our index by comparing the news content in these tweets to a corpus of "[...] authoritative texts on the subject of climate change" as in Engle et al. (2020). Similar to Engle et al. (2020), we aggregate the authoritative text documents into a Climate Change Vocabulary (CCV), which amounts to the list of both unique terms and their associated frequency with which each one of them appears in the aggregated corpus. In the construction of our dataset, we use the text (if any) of the Twitter posts and not the

[1]Our data collection ended in December 2022. The platform is currently identified as "X". The list of newspapers included in our data set can be found in the appendix. The selection of newspapers was determined through a two-step process: first, we verified whether the newspapers had been included in prior studies (Baker et al. 2016) and were categorized as primary information outlets. Second, we expanded upon this criterion by evaluating whether each newspaper's Twitter handle had a substantial number of followers and maintained consistent posting activity.

TABLE 1. DATASET SUMMARY

Country	Tot. no. News Outlets	Tot. no. Tweets	Tot. no. Words	Tot. no. Terms	Language
AR	4	1,892,464	16,592,918	50,513	Spanish
AU	4	539,792	5,805,411	46,253	English
BR	3	1,091,173	9,157,179	46,841	Portuguese
CA	5	1,071,360	9,662,873	48,695	English
CH	4	312,897	2,477,651	40,932	German and French
CL	3	1,088,455	9,422,589	48,409	Spanish
CN	3	488,076	6,786,626	53,342	English
CN (HK)	2	305,490	2,982,160	28,143	English
CO	3	1,291,773	10,348,974	55,984	Spanish
DE	4	708,692	6,779,556	31,190	German
ES	4	1,484,502	13,662,696	61,176	Spanish
FR	4	1,004,595	8,950,751	54,021	French
IN	4	1,909,474	22,370,252	71,505	English
IT	3	1,268,190	10,209,216	42,084	Italian
JP	4	353,247	3,819,349	36,544	English
KR	4	302,946	2,814,363	28,923	English
MX	4	2,041,505	19,553,684	70,880	Spanish
NO	3	152,521	921,258	13,022	Norwegian
NZ	3	147,218	1,156,784	20,538	English
PT	3	802,011	6,102,651	40,929	Portuguese
SA	3	914,623	8,754,709	44,571	Arabic
SE	4	190,493	1,607,852	19,201	Swedish
UK	4	791,929	6,978,125	46,460	English
US	11	2,735,338	29,141,511	72,662	English
ZA	3	453,135	3,945,579	33,473	English
Total	**96**	**23,341,899**	**220,004,717**	**1,106,291**	

Notes: This table shows summary statistics for all news that we collect for a large cross section of countries. Our real-time data range from 1/10/2014 to 31/12/2022. For each country, we report the total number of Twitter accounts that we monitor (major newspapers and other media outlets), the total number of tweets collected, total number of words, total number of unique terms (accounting for unigrams and bigrams), and original language. We translated the corpus in Engle et al. (2020) to 8 different languages, in order to construct our index.

respective articles. Before doing so, we preprocess both the corpus of authoritative texts and the newspaper's tweets. The preprocess removes (1) any links, (2) any tags to Twitter accounts, (3) any special characters and/or numbers, and (4) stop words (e.g, "and" "or"). Furthermore, it stems each word (using the Snowball algorithm),

and it keeps only words with more than two characters. The stemming procedure retains only the root of each terms; for example, terms like "work" and "working" are included as unique terms. See Figure A.1 in the appendix for a word cloud representation of the preprocessed corpus in English.

Second, we construct the analogous count from our preprocessed Twitter texts for every country. Our approach enables us to construct our measures both at high and low frequency. When studying the impact of climate attention shocks on currencies, we use a daily aggregation method. In what follows, we focus on monthly aggregation of tweets for illustrative purposes. We refer to the Twitter texts aggregated in a specific month for a specific country as "document". At the monthly frequency, we have a total of 99 documents for each country. Next, we convert the term counts from each one of our documents into term frequency–inverse document frequency scores (in short, "tf-idf" scores). Finally, for each document, we compute the cosine similarity between its tf-idf scores and those of the entire corpus. We carry out the described procedure for every country within our sample.

In cases where a country uses a language other than English, we employ the Google Translate API to translate the original English corpus into the appropriate foreign language. These languages include German, Spanish, French, Norwegian, Swedish, Arabic, Portuguese, and Italian. This approach enables us to create Climate Change Vocabulary (CCV) sets for each of the available languages, facilitating the analysis of newspapers published in local languages. This approach mitigates the potential news bias that might arise from solely relying on English-language newspapers in non-English-speaking countries.[2] For countries with multiple local languages, such

[2]For China, Japan and Korea, we retained the English-speaking newspapers posts due to the challenges in preprocessing languages with special characters. Our results are robust to the removal of these countries.

as Switzerland, we generate an index for each language and calculate the average across these indices.

Figure 1 presents our weekly Climate Attention Index (CAI), which has been aggregated across countries. The index is constructed by taking the equally weighted average across all the countries in our sample. The calculation of the index at the country-level is necessary because we cannot mix documents written in different languages. Consolidating documents at the country-language-frequency level would yield highly comparable results.

Our index effectively reflects specific global events. For instance, the United Nations Climate Change Conference (COP26), held in early November 2021 with the aim of promoting commitments to combat climate change, garnered significant attention worldwide, as evident in our index. Conversely, the COVID-19 pandemic and the invasion of Ukraine had the opposite effect on our index, with a notable decline attributed to a reduced proportion of climate-related discussions during these periods. Typically, significant events like elections, conflicts, and health crises tend to lead to a decrease in our index.

Figure 2 illustrates the same index across all of the countries included in our dataset. One of the novelties of our dataset is that it spans a large cross-section, which enables us to measure heterogeneity across countries. In the spirit of the international macro-finance literature, in what follows we focus primarily on heterogeneous exposures to global shocks (see Lustig et al. (2011)).

Specifically, let $CAI_{i,t}$ denote the index for country i at time t. The world climate

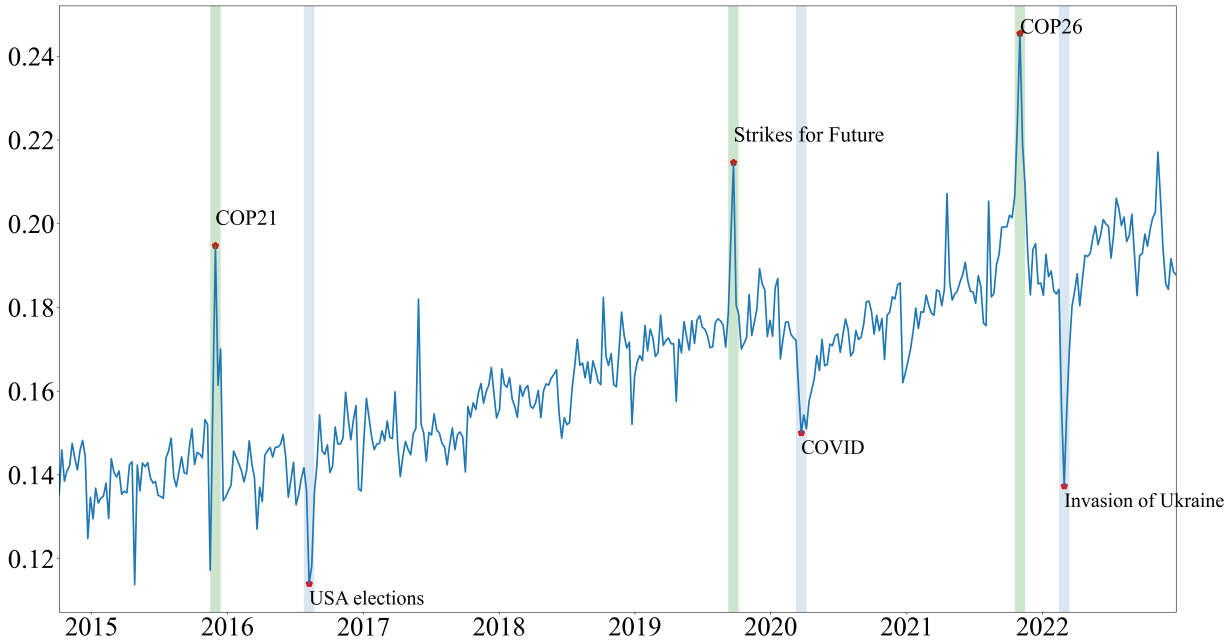


FIG. 1. WORLD CLIMATE ATTENTION INDEX (CAI)

Notes: This figure shows our Global Climate Attention Index. It is based on the methods described in section 2 applied to the countries listed in table 1 and a total of 8 languages.

attention index is defined as follows:

$$\overline{CAI}_t = \sum_i \omega_{i,t} CAI_{i,t}, \tag{1}$$

where $\omega_{i,t}$ is a country-specific weight. We provide results based on three alternative weighting schemes: (i) by equally weighting all countries, (ii) by weighting each country proportionally to its share of global GDP, and (iii) by weighting each country proportionally to its share of Twitter volume. Volume weights are based only on tweets with a similarity score with the corpus of authoritative text above median. Equivalently, we only include the volume of tweets that are the most relevant for the focus of our analysis. We then estimate the following regression:

$$\Delta CAI_{i,t} = \beta_i \cdot \Delta \overline{CAI}_t + u_{i,t}, \tag{2}$$

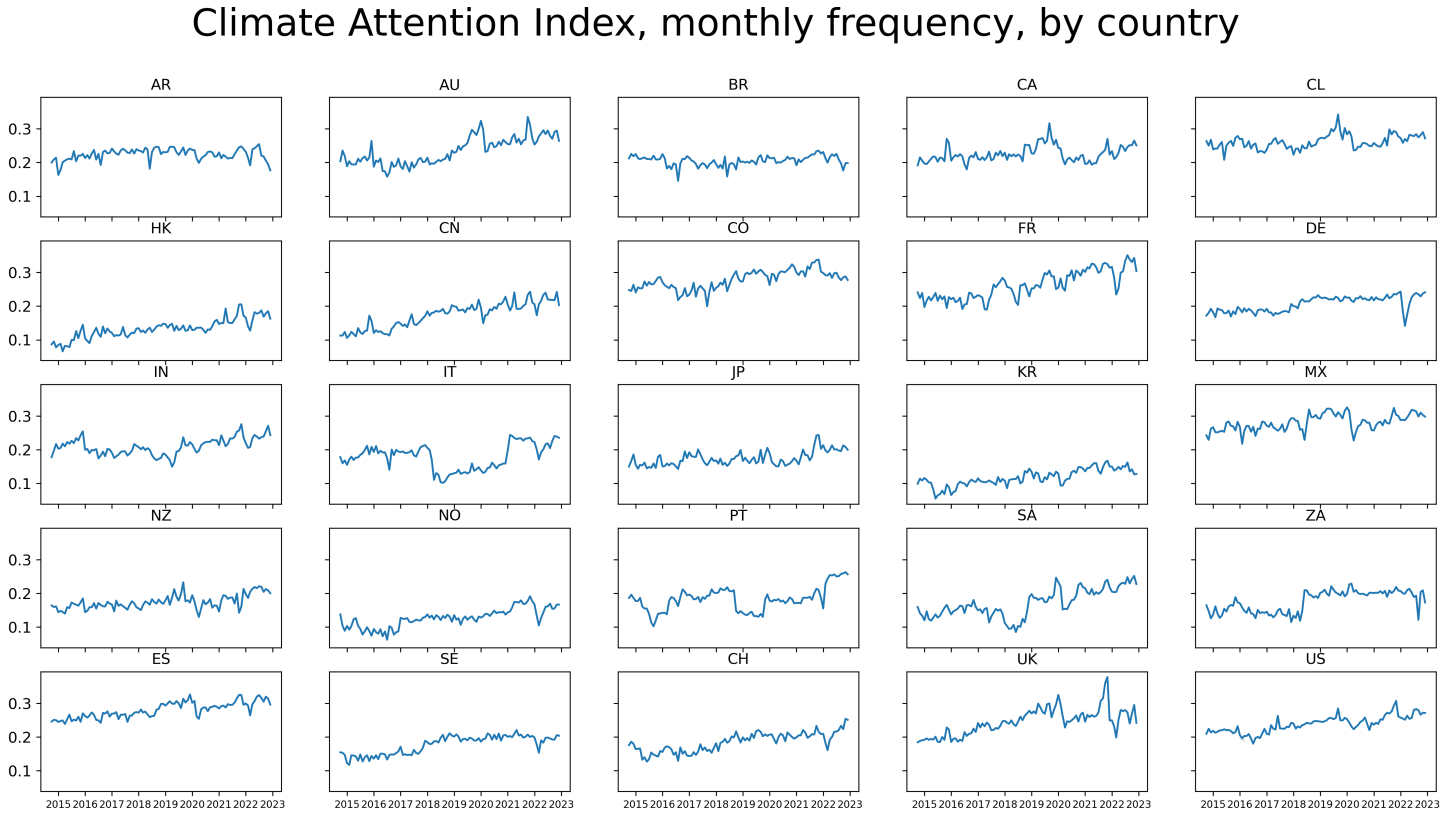


FIG. 2. WORLD CLIMATE ATTENTION INDEX (CAI) BY COUNTRY

Notes: This figure shows our Global Climate Attention Index. It is based on the methods described in section 2 applied to the countries listed in table 1 and 8 languages. For countries with multiple languages (e.g., Switzerland), the country-level index is the average of each language index.

where Δ refers to a demeaned growth rate over time for each country. We regard β_i as a measure of exposure to a common, i.e., global, component, and $u_{i,t}$ as a pure local component.

Table 2 presents the estimated β parameters for each country in our sample under various weighting schemes for the global CAI index. These β values exhibit a strong positive correlation across different weighting schemes, with correlation coefficients exceeding 0.9. Using the equally weighted global CAI index as the reference, we observe that South Korea, Saudi Arabia, China (including both Hong Kong and Mainland), and Japan consistently possess the highest β values. This aligns with expectations, as some of these countries are typically perceived as being more susceptible to climate change impacts (see for example, Hijioka et al. (2014), Pigato and Stewart (2020), and Sun et al. (2022)), reinforcing the credibility of our indices. Conversely, Switzerland, South Africa, Chile, Norway, and Germany consistently exhibit the lowest β values, indicating their relative resilience to climate change effects.

Top days. In the next section, we use high-frequency data to identify the impact of climate news shocks on exchange rates and stock returns. To identify innovations in our global index, we initially calculate the daily growth rate in the raw CAI index for each country and subsequently remove its mean. These demeaned indices at the country level are then winsoried at the 99.9% and aggregated to generate a global metric.[3] The outcomes of this analysis are visualized in Figure 3.

Based on the distribution of innovations in our global climate index, we select the top 15% of these innovations.[4] Specifically, we examine the reaction of currencies

[3]When we compute our index at the daily frequency, it is possible that in some days and for some countries we could have extreme growth rates because our index gets close to zero. We remove both the top- and bottom-0.1% realizations from our sample.

[4]We analyze the distribution of news for each day of the week, which allows us to account for any

TABLE 2. ESTIMATED β FOR EACH COUNTRY

	Equally weighted		GDP weighted		Volume weighted	
Country code	β	s.e.	β	s.e.	β	s.e.
AR	0.929	0.209	0.574	0.148	1.047	0.246
AU	1.419	0.197	0.932	0.190	1.375	0.219
BR	0.616	0.293	0.470	0.218	0.717	0.294
CA	1.710	0.224	1.312	0.138	1.789	0.232
CL	0.241	0.285	0.113	0.175	0.262	0.291
CN (HK)	2.105	0.325	1.196	0.326	1.619	0.518
CN	2.014	0.344	1.787	0.142	1.887	0.450
CO	0.679	0.180	0.561	0.115	0.702	0.207
FR	0.662	0.247	0.320	0.243	0.712	0.274
DE	0.363	0.122	0.236	0.074	0.316	0.160
IN	1.410	0.367	1.144	0.184	1.547	0.330
IT	0.985	0.593	0.624	0.473	1.441	0.705
JP	1.895	0.271	1.472	0.236	1.750	0.233
KR	2.413	0.394	1.624	0.280	1.889	0.324
MX	0.613	0.243	0.376	0.141	0.847	0.244
NZ	0.811	0.293	0.428	0.223	0.767	0.318
NO	0.344	0.320	0.245	0.267	0.166	0.313
PT	0.469	0.663	0.083	0.432	0.130	0.614
SA	2.266	0.574	1.108	0.251	2.254	0.609
ZA	0.197	0.466	-0.029	0.466	0.063	0.612
ES	0.534	0.128	0.366	0.084	0.578	0.114
SE	0.592	0.251	0.255	0.116	0.394	0.208
CH	-0.028	0.414	-0.014	0.263	-0.168	0.335
UK	0.993	0.269	0.798	0.214	0.998	0.339
US	0.768	0.143	0.743	0.083	0.905	0.134

Notes: This table reports the estimated β_i reported in equation (2), that is, the country-specific exposure to the global climate attention shock. The global climate attention shock is constructed as the equally weighted, GDP-weighted, and Twitter volume-weighted cross-sectional average at each point in time. Volume- and GDP-based weights are lagged by one period. The sample ranges from 2015:Q1 to 2022:Q4. Standard errors are HAC-adjusted.

and stocks in the days following a substantial increase in climate attention. This approach serves two purposes: (i) to minimize noise from news unrelated to climate,

patterns specific to particular days (e.g., Monday or Friday effects). This approach is standard in studies focusing on daily news.

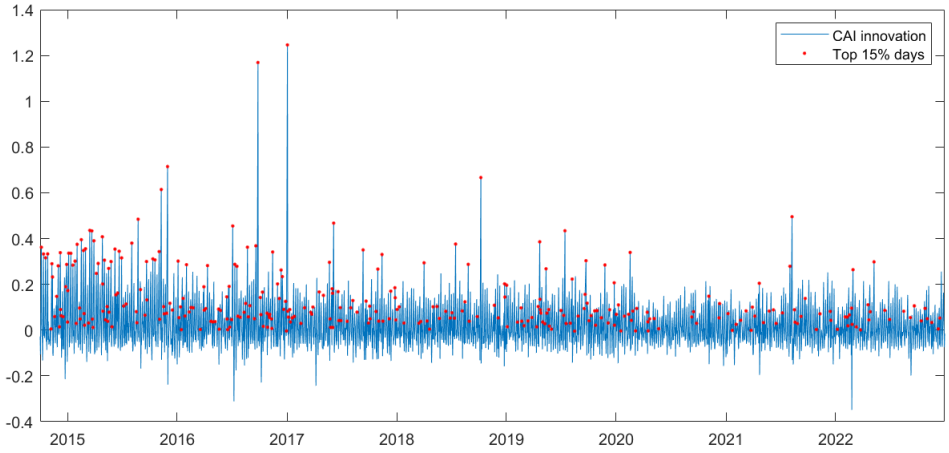


FIG. 3. INNOVATIONS TO WORLD CLIMATE ATTENTION INDEX (CAI)

Notes: This figure shows innovations to our equal-weights Global Climate Attention Index constructed as described in section 2. Our cross section of countries is reported in table 1. Country-level indices are aggregated using equal weights. Red dots are classified as climate-related news days (top-15% realizations). Weekends are excluded.

and (ii) to more effectively identify days driven by "pure" climate news shocks. Such a methodology is commonly used in the literature investigating the effects of news related to policy announcements (see, for instance, Leombroni et al. (2021)). It is worth noting that some days with a high volume of climate-related news may fall below our top 15% threshold due to the dominance of other topics in the news. As a result, similar to previous studies, this procedure may introduce a downward bias, making it less likely to detect a significant effect of climate news on asset prices and currencies.

Topics for top days. After identifying top-attention days, we examine the content of the news shared during these periods. Following the text analysis literature (see, for example, Hassan et al. (2019)), we employ a pre-trained sentence embedding model to extract semantic representations of newspaper tweets. These embeddings are then clustered to identify a smaller set of key themes, or main topics. This dimen-

sionality reduction enables the use of topic-level cosine similarity scores to classify tweets as climate-related and further distinguish between those primarily associated with physical risk and transition risk. The process involves several carefully designed steps aimed at minimizing discretion on our part, which we detail below.

First, we generate 100 climate risk-related sentences using ChatGPT: 50 focused on physical risks (e.g., extreme weather) and 50 on transition risks (e.g., regulatory changes). The full list of these sentences is provided in Table A.2 in the Appendix. Next, we analyze the identified top climate-attention days by preprocessing raw newspaper tweets, removing non-informative elements such as links and special characters. We then convert the cleaned tweets into high-dimensional vector representations (sentence embeddings), which serve as inputs for the BERTopic clustering algorithm (see Grootendorst (2022)).[5]

After identifying the key topics discussed in the media on these top-attention days, we compute cosine similarities between each topic embedding and each AI-generated sentence embedding. This approach allows us to assess how closely each topic aligns with climate-related themes. Specifically, a topic is classified as climate-related if its cosine similarity score with any AI-generated climate sentence falls within the top 0.1% of the score distribution (with a threshold of 0.546). Using the 99.9^{th} percentile ensures a stringent definition of climate-related topics.

Finally, we classify each climate-related topic as either "Physical Risk" or "Transition Risk" based on its closest match to the sentences listed in Table A.2. If the most

[5]BERTopic is a topic modeling technique that integrates transformer-based embeddings with clustering to extract coherent topics from large text datasets. We use the package provided at https://maartengr.github.io/BERTopic/index.html. We keep the following default options: (i) UMAP (Uniform Manifold Approximation and Projection) with five components, and (ii) HDBSCAN (Hierarchical Density-Based Spatial Clustering of Applications with Noise) to group tweets into distinct topics. Since our data comprise tweets in different languages, we must use the embedding model "distiluse-base-multilingual-cased-v2" by Reimers and Gurevych (2019).

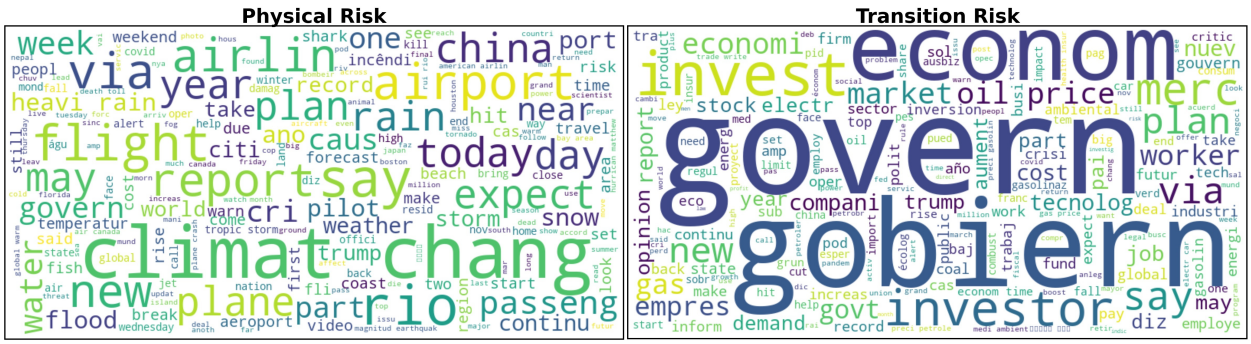


FIG. 4. WORDCLOUD OF CLIMATE-RELATED TWEETS DURING TOP DAYS.

Notes: This figure shows the word cloud of root words extracted from climate-related Tweets in our sample of top days. Tweets are classified as climate-related if the cosine similarity of their associated topic exceeds the 99.9th percentile of the similarity scores calculated against a set of AI-generated reference sentences. Tweets are further classified as physical (transition) risk if their topic aligns most closely with a physical (transition) risk-related sentence (see table A.2). Our sample period starts in October 2014 and ends in December 2022. Transition risk generally refers to risks arising from changes in policies, technologies, and market preferences associated with climate action. Physical risk relates to the direct impact of climate change, such as extreme weather events and rising temperatures.

related sentence corresponds to physical (transition) risks, the topic is labeled accordingly. Figure 4 visualizes the most frequent words in these two groups of tweets, with the resulting word clouds reinforcing our methodology by clearly distinguishing between different sources of climate-related concerns. In the following analysis, we use these two groups of tweets in both our sentiment analysis and high-frequency asset pricing analysis.

Sentiment of tweets. We analyze the sentiment of climate-related tweets during top days by using the Twitter-XLM-RoBERTa model from CardiffNLP.[6] This is a transformer-based multilingual sentiment classifier suitable for text in multiple languages (Barbieri et al. 2022). Each one of our tweets is tokenized and passed through the pre-trained model in order to obtain a sentiment label (negative, neutral, or positive) based on the highest logit value.

[6]Available at https://huggingface.co/cardiffnlp/twitter-xlm-roberta-base-sentiment.

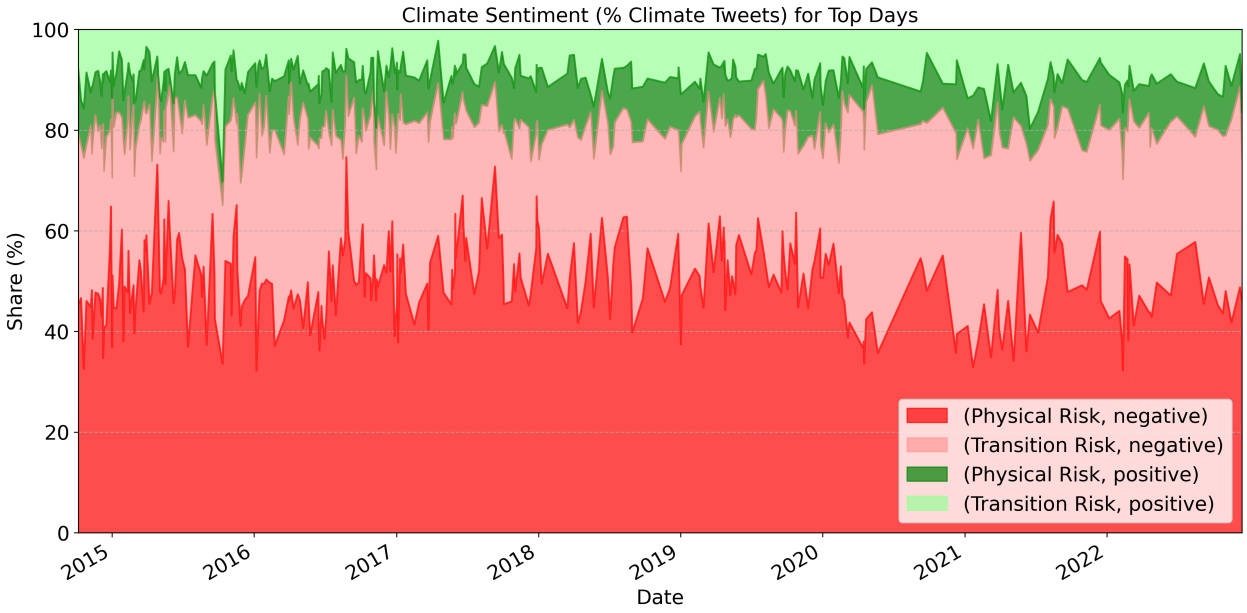


FIG. 5. SENTIMENT OF CLIMATE RELATED TWEETS DURING TOP DAYS.

Notes: This figure presents the share of climate-related tweets categorized by sentiment (positive or negative) and risk type (transition or physical) on days for which there is a positive spike (top-15%) in the global CAI innovations. The sentiment classification is based on a multilingual sentiment classifier Barbieri et al. 2022). The word clouds for transition and physical risk risk are reported in figure 4.

Figure 5 presents the share of climate-related tweets in each risk category (physical and transition) that are classified as either positive or negative. In our sample, global news shocks related to climate typically have a negative tone. Equivalently, our top-attention days are usually bad-news days.

Attention vs vulnerability. To further analyze our text-based indices, we assess the correlation between our estimated β values and alternative measures of climate exposure. We first use the vulnerability score provided by the Notre Dame Global Adaptation Initiative. This index aims to encapsulate "a country's exposure, sensitivity, and capacity to adapt to the negative effects of climate change." We calculate the average of these scores over the longest available period (1995-2021). The upper panel of Figure 6 illustrates the relationship between our β estimates and the vulner-

ability score. We observe a positive and statistically significant correlation between our β estimates and this index, implying that countries with greater susceptibility to climate change usually exhibit higher β values, i.e, more attention exposure to global climate news.

Second, we relate our estimated β values to absolute latitude. Generally, countries situated in regions with higher absolute latitudes are usually considered less exposed to rising temperatures resulting from climate change. To assess this, we compile a dataset of city-level absolute latitudes for each country and compute the population-weighted average of these latitudes. Our analysis reveals a negative correlation between our β estimates and absolute latitude, reinforcing the effectiveness of these estimates in capturing a country's exposure to climate change.

Importantly, we observe that both absolute latitude and the vulnerability index account for a moderate portion of the cross-sectional dispersion of our β coefficients. This indicates that our exposure measure is not fully captured by other existing indicators. In the next section, we will show that our exposure coefficients provide additional information beyond what is captured by vulnerability.

3 Climate news shocks in a no-arbitrage model

In this section, we use a no-arbitrage approach to derive a set of hypothesis that we test in our novel dataset.

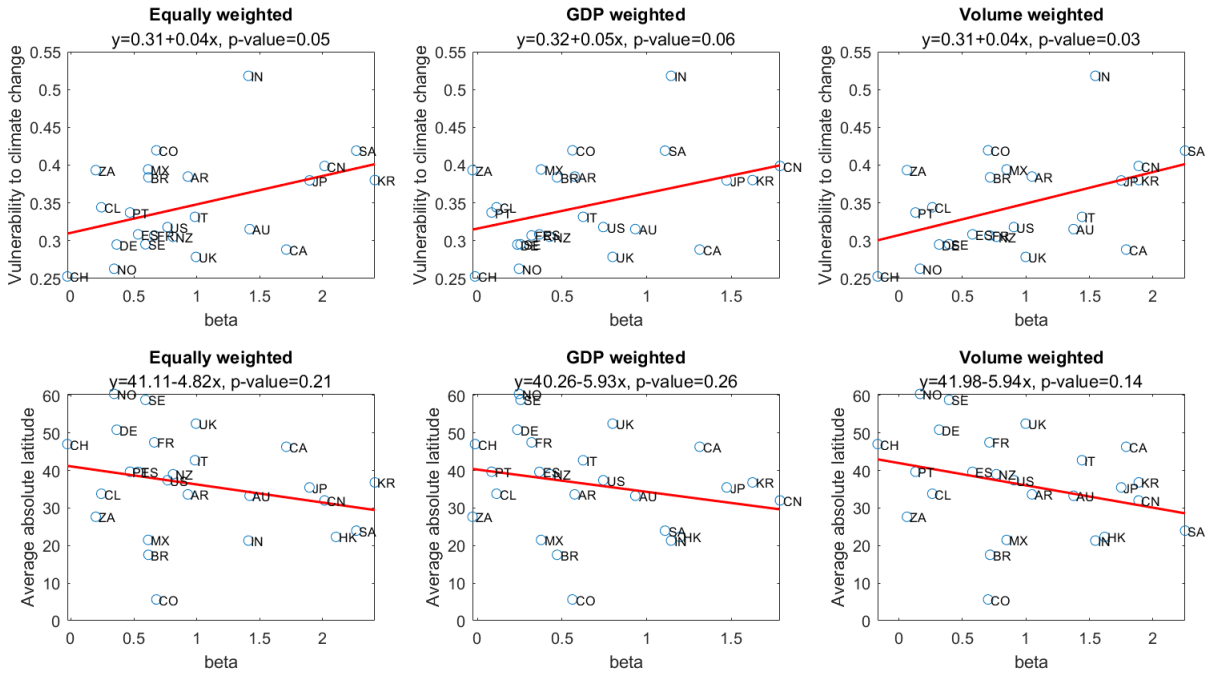


FIG. 6. β AGAINST VULNERABILITY TO CLIMATE CHANGE.

Notes: This figure shows the scatter plot of the estimated βs in equation (2), and measures of vulnerability to climate change across countries. The βs are estimated using the global climate attention shock constructed as either the equally-, GDP-, or Twitter volume-weighted cross-sectional average at each point in time. The upper panels consider each country's average vulnerability score from the Notre Dame Global Adaptation Initiative. The lower panels refer to the average absolute latitude of each country, that is, a population-weighted average absolute latitude of all cities in each country. City-level latitudes are collected from the World Cities Database.

3.1 Exchange Rates

Consider a complete market model with two countries, A and B, each populated by a representative investor. Assume that the stochastic discount factors in log-units are:

$$m_{A,t} = \bar{m} + \beta_A \cdot \epsilon_t, \quad m_{B,t} = \bar{m} + \beta_B \cdot \epsilon_t,$$

where positive realizations of ϵ_t represent common, i.e., global, bad news shocks about climate. If markets are complete, the percentage variation in the exchange rate can

be expressed as follows:

$$\Delta e_{(A,B),t} = m_{A,t} - m_{B,t} = (\beta_A - \beta_B)\epsilon_t.$$

Here $\Delta e_{(A,B)} > 0$ refers to an appreciation of the currency of country A. In what follows, we assume that $\beta_A > \beta_B$, so that–by no arbitrage–adverse global climate news shocks should imply an appreciation of the currency of the most exposed country.

In order to test this condition, we obtain bilateral exchange rate data from Bloomberg and sort our country pairs as follows. Let A and B be two countries in a country-pair. For every non-repeated pairwise combination of countries, $i \neq j$, we look at the exposure of the country-specific CAI to the global CAI as estimated in equation (2). If $\beta_i - \beta_j > 0$ ($\beta_i - \beta_j < 0$) we denote country i as A and j as B (j as A and i as B) and focus on the exchange rate $e_{(A,B)}$.

We test this assumption at a high-frequency level, particularly on days when climate-related news is exceptionally significant. Figure 7 illustrates the average cumulative exchange rate variation following these specific days,

$$\Delta e_{t,t+k} := \sum_{s=0}^{k-1} \Delta e_{t+s,t+s+1} \frac{100 \cdot N^{top}}{k}.$$

Cumulative returns are averaged over the time horizon k, they are in percentage, and they are multiplied by N^{top}, i.e., the average number of top-days in a year. In our benchmark analysis $N^{top} = 38$.

To ensure that our observations are not influenced by idiosyncratic patterns in our dataset, these averages are computed relative to the average cumulative variation observed in the remaining 85% of business days in our sample. Specifically, we estimate

the relative cumulative returns with the following regression:

$$\Delta e^{i,j}_{t,t+k} = a^{i,j}_k + b_k \cdot \mathbb{1}^{Top}_t + \epsilon^{i,j}_{t,k},$$

where $\mathbb{1}^{Top}_t$ is a dummy variable that equals 1 if the day falls in the set of extreme climate news days. b_k captures the relative cumulative returns over a horizon of k days. We only include country pairs where β_i is significantly larger than β_j at 10% level (see figure B.1, Appendix B). Standard errors are clustered at both the date and country-pair level.

If climate-related news has no bearing on exchange rates, we would anticipate null cumulative effects. Conversely, our findings reveal that adverse climate news shocks are linked to the contemporaneous appreciation of countries that are comparatively more exposed (i.e., possessing higher β values). Furthermore, this appreciation exhibits persistence and it extends over multiple days, signifying a lasting impact on currencies.

In Figure 8, we illustrate this effect among pairs of countries consisting solely of advanced economies (left panel), developing economies (right panels), or a combination of advanced and developing countries (middle panel).[7] The appreciation pattern is observed across all country pairs. Furthermore, it tends to persist longer when at least one emerging country is involved in the analysis.

Robustness. In Appendix B, we show that our results are unchanged when we focus on either a GDP-weighted global index (figure B.2(a)) or a Twitter volume-

[7]We define advanced economies according to the IMF, where the advanced economies in our sample are: AU, CA, CN (HK), FR, DE, IT, JP, KR, NZ, NO, PT, ES, SE, CH, UK, US. The developing economies are: AR, BR, CL, CN, CO, IN, MX, SA, ZA.

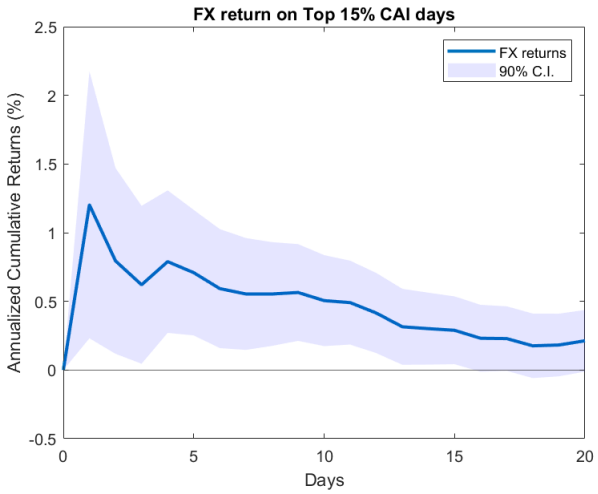


FIG. 7. FX AND INNOVATIONS TO WORLD CLIMATE ATTENTION INDEX (CAI)

Notes: This figure shows the average cumulative return in exchange rates around days with a positive spike (top-15% days in our sample) in the global CAI. This cumulative variation is net of the common cumulative variation that we obtain when considering all other days in our sample. Exchange rates are computed at Greenwich Mean Time in each day across 138 country pairs with exposures to the global CAI that are different from each other at the 10% confidence level. Exchange rates are quoted such that for each country pair an appreciation refers to the country with the higher exposure to global climate news shocks. Our Global Climate Attention Index is based on the methods described in section 2. Countries are equally weighted. The shaded areas present the 90% confidence interval which is constructed using standard errors clustered at both the date and country-pair level.

weighted global index (figure B.2(b)). We also replicate the same exercise by focusing on GDP- and Volume-weighted CAI indeces (figures B.2(a)-B.2(b)). Our results are qualitatively unchanged. In addition, if we change the threshold of top days from 15% to either 10% or 20%, our results remains unchanged (figures B.3(a)-B.3(b)).

Figures B.4(a)-B.4(b) confirm that our results are not sensitive to the choice of the significance level that we use in order to select country-pairs with different exposure coefficients. Our results apply regardless of whether we include all country pairs (including those with modest heterogeneity in beta) or just those with a more pronounced degree of heterogeneity (5% confidence level).

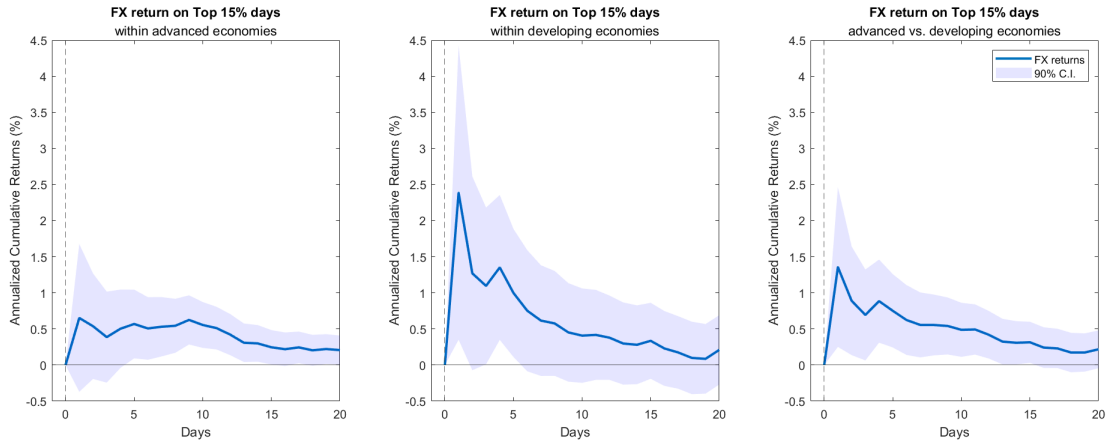


FIG. 8. FX AND INNOVATIONS TO WORLD CAI ACROSS COUNTRY PAIRS

Notes: This figure shows the average cumulative return in exchange rates after days with a top-15% positive spike in the global CAI. For more details, see the notes under figure 7 and section 2. We focus on country pairs in which (i) both countries are advanced economies (left panel), (ii) only one country is defined as an advanced economy (mid panel), and (iii) both countries are developing economies (right panel).

Figure B.5(a) shows that our results are confirmed also when we aggregate the five Euro Area countries in our datatset (DE, FR, IT, PT, ES) into a single entity with a common currency. Most importantly, figure B.5(b) confirms that our results are not driven by vulnerability, but rather by the unique information content of our estimated exposure coefficients. Specifically, we orthogonilize our exposure coefficients with respect to vulnerability by considering the residuals of the cross sectional regression depicted in figure 6. The results in figure B.5(b) are based on the residual exposure and are consistent with our benchmark results. Equivalently, using heterogeneity in vulnerability across countries produces insignificant responses. The same conclusions apply to absolute latitude.

Figure B.6(a) confirms our main findings when using exposures estimated at the monthly frequency. Figure B.6(b) is constructed as figure 7 in main text, but it uses weekly observations and it includes weekends. The resulting weekly CAI index covers a total of 430 weeks. During this process, climate-related tweets are aggregated

on a weekly basis, with each week of the time series commencing on a Saturday. This weekly aggregation provides a comprehensive perspective on climate-related discussions in social media, encompassing an extended period that includes weekends.[8] Similar to our daily frequency analysis, we identify weeks in which our index records top values and evaluate their cumulative impact on exchange rates.

In Figure B.7 in the appendix, we show the results from the following regression,

$$\Delta e^{i,j}_{t,t+k} = a^{i,j}_k + (b_k + c_k \cdot S_t) \cdot \mathbb{1}^{Top}_t + \epsilon^{i,j}_{t,k}, \tag{3}$$

where S_t denotes the share of tweets talking about transition risks at day t, normalized between 0 and 1. This specification enables us to identify whether our results are primarely driven by transition of physical risk. We find that the results depicted in figure 7 are consistent with those obtained by estimating equation (3) and setting S_t to its median value. Most importantly, we find that the results are stronger when $S_t = 1$, i.e., in top days when attention is entirely about transition risk. Thus transition risk seems to be the main driver of currency reactions.

In Figure B.8, we examine local top-attention days, as opposed to global top-attention days. We find that local shocks have no significant impact on FX markets. More broadly, local shocks also appear less relevant in the equity analysis presented next. For brevity, we exclude local shocks from the subsequent analysis.

[8]To identify the top weeks in terms of climate attention, we calculate the growth rate of the weekly global CAI, then the top 10% of observations of this time series are considered as indicative of heightened climate attention. We only keep top weeks that are at least 5 weeks apart to avoid the confounding effects.

3.2 Equity returns

Based on our findings related to currencies, we investigate the effects of our climate news index on equity returns denoted in USD. Specifically, we examine the behavior of average cumulative returns following days marked by a positive spike in our global index (CAI), taking into account both stock-specific exposure and country-specific conditions.

We use emission intensity as a proxy for stock-specific exposure, defined as emissions in tons of CO2 divided by sales. We source annual data on emission intensity from the Trucost dataset. For country-specific conditions, we use sensitivity coefficients denoted by β, as reported in table 2. Our dataset includes 16,774 firms and totals 23,305,563 firm-day observations. We estimate the following regression:

$$r^{i,c}_{t,t+k} = \alpha^i_k + \zeta^{i,c}_{t,k} \cdot \mathbb{1}^{Top}_t + \epsilon^{i,c}_{t,k}, \tag{4}$$

$$\zeta^{i,c}_{t,k} = \gamma_{0,k} + (\gamma_{1,k} + \gamma_{2,k} \cdot \beta_c) \cdot E_{i,t_a}, \tag{5}$$

where c denotes the country in which the headquarter of the firm is located, i refers to one of our firms, β_c represents our equally weighted sensitivity, E_{i,t_a} is the emission intensity of firm i assessed the year prior to day t, and $\mathbb{1}^{Top}_t$ is a dummy variable that equals 1 if the day falls in the set of extreme climate news days. In equation (4), the left-hand side variable is defined as follows:

$$r^{i,c}_{t,t+k} = \sum_{s=0}^{k-1} r^{i,c}_{t+s,t+s+1} \frac{100 \cdot N^{top}}{k},$$

that is, it is averaged over the time horizon k, it is in percentage, and it is multiplied by the average number of top-days in a year.

Since emission intensity is very persistent at the annual frequency, the coefficient $\zeta_{t,k}^{i,c}$ is almost time-invariant in our dataset. Consequently, this composite coefficient primarily reflects heterogeneity across different countries and stocks. The literature has proxied the exposure of a firm to climate risk either by examining its emissions or considering geographical factors such as distance from the ocean or latitude. We hypothesize that a firm's equity returns' sensitivity to climate news reflects a convolution of its emission levels (as measured by total emissions) and the degree of investor attention to climate news within a specific country (as captured by our country-level β).[9] We are particularly interested in the interplay of these dimensions, as negative global climate news could be concentrated only among firms with high emissions in highly exposed countries ($\gamma_{2,k} < 0$). Our estimates confirm this intuition. In figure 9, we depict the estimates of our composite parameter $\hat{\zeta}_{t,k}^{i,c}$ over different daily horizons, k.

In the top portion of the figure, we first sort countries according to their exposure β. The top-decile of the distribution of βs is 2.27 (Saudi Arabia). The bottom-decile is 0.197 (South Africa). We then select the values of carbon emission intensity for a representative green (brown) firm using the 5th (95th) percentile of the emission intensity distribution, which corresponds to the median value within the top-decile (bottom-decile).[10] Given these numbers, we can depict the implied estimated composite coefficient $\zeta_{t,k}^{i,c}$ and its associated standard error across different daily horizons, k.

The bottom two panels convey the same information as the top panels but from a different perspective. Specifically, the bottom left (right) panel presents the composite

[9] This approach amounts to conjecturing that a brown firm in a country subject to floods may be subject to stronger valuation effects than an equally brown firm in a country whose climate is expected to improve due to global warming.

[10] The 5th (95th) percentile of the log emission intensity in our sample is 0.43 (6.88). The thresholds remain consistent both across and within countries because the country-level distribution of emission intensities is stable. See figure B.9 in the appendix for more details.

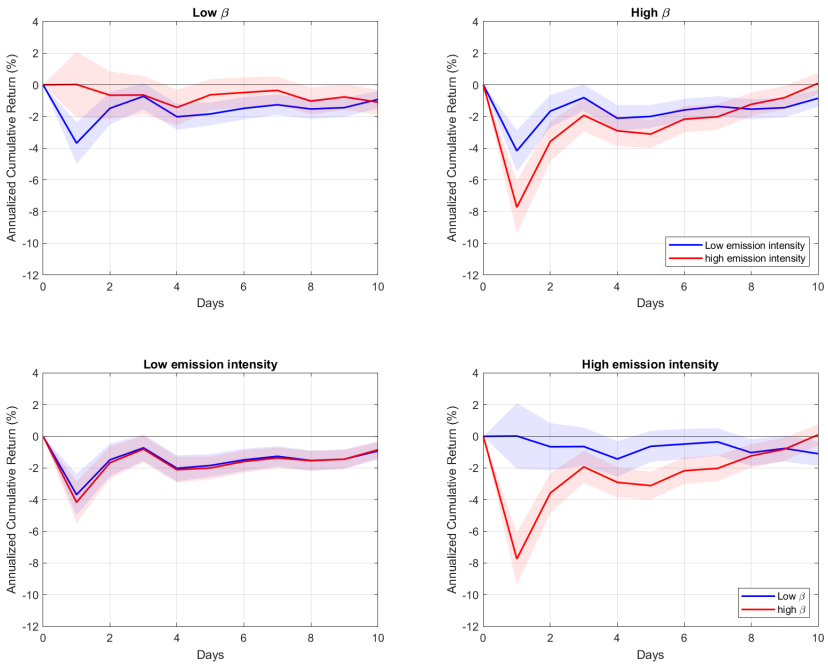


FIG. 9. USD EQUITY RETURNS AND INNOVATIONS TO WORLD CAI

Notes: This figure shows the average cumulative return in equity returns after days with a top-15% positive spike in the global CAI. For more details, see the notes under figure 7. We depict the estimates of $\zeta_{t,k}^{i,c}$ as defined in equations (4)-(5) across different daily horizons, k. Standard errors are clustered at the industry×date and firm level. We follow the Fama-French 49 classification. The sample comprises a total of about 23 million firm-day observations. Daily returns are annualizedusing the average number of top climate days in a year. In the four panels, high (low) β refers to the top-decile (bottom-decile) of betas across countries in our sample, and high (low) emission intensity is using the top- and bottom-5% of emission-sorted firms in our sample. The shaded areas present the 90% confidence interval.

coefficients for a representative green (brown) firm in a low-β country and in a high-β country.

Our analysis yields several significant findings. Firstly, firms situated in countries with moderate exposure to our global CAI tend to experience a more moderate loss of value. This effect holds for both high- and low-emission firms. Conversely, firms in countries with high β values suffer a more severe loss of value, an effect that is particularly pronounced for high-emission firms. Across all these scenarios, the

negative impact on cumulative returns is very persistent.

Changing the order of the sorting variables does not alter our conclusions. Specifically, the bottom two panels of figure 9 confirm that firms located in 'naturally hedged' countries (that is, countries with low β) are generally less affected by adverse climate news. However, when examining stocks with high emission intensity, the negative impact on valuation is more severe for firms in countries with a higher climate news β.

Following our analysis of currency markets, we examine whether these results are primarily driven by top-attention days in which news focuses on either physical or transition risk. Specifically, we estimate the following specification:

$$\begin{aligned} r^{i,c}_{t,t+k} &= \alpha^i_k + \zeta^{i,c}_{t,k} \cdot 1^{Top}_t + \epsilon^{i,c}_{t,k}, \\ \zeta^{i,c}_{t,k} &= (\gamma_{0,k} + (\gamma_{1,k} + \gamma_{2,k} \cdot \beta_c) \cdot E_{i,t_a}) + (\kappa_{0,k} + (\kappa_{1,k} + \kappa_{2,k} \cdot \beta_c) \cdot E_{i,t_a}) \cdot S_t, \end{aligned}$$

where S_t represents the share of tweets discussing transition risks on day t, normalized between 0 and 1. Figure B.13 in the appendix presents our results. The responses are constructed using the composite coefficient $\zeta^{i,c}_{t,k}$, with $S_t = 0.50$ in the left panel and $S_t = 1$ in the right panel. For a median top-attention day, this specification reproduces the results reported in Figure 9. When news is primarily about transition risk, we observe more pronounced depreciations across all panels. As with currency markets, equity depreciations are largely driven by negative news on transition risk. Notably, the response of equity returns to these news events appears homogeneous across countries with varying exposure and across firms with different emissions. This finding suggests that (i) regulation-related interventions may have broadly similar effects across firms, and (ii) our benchmark result—where brown

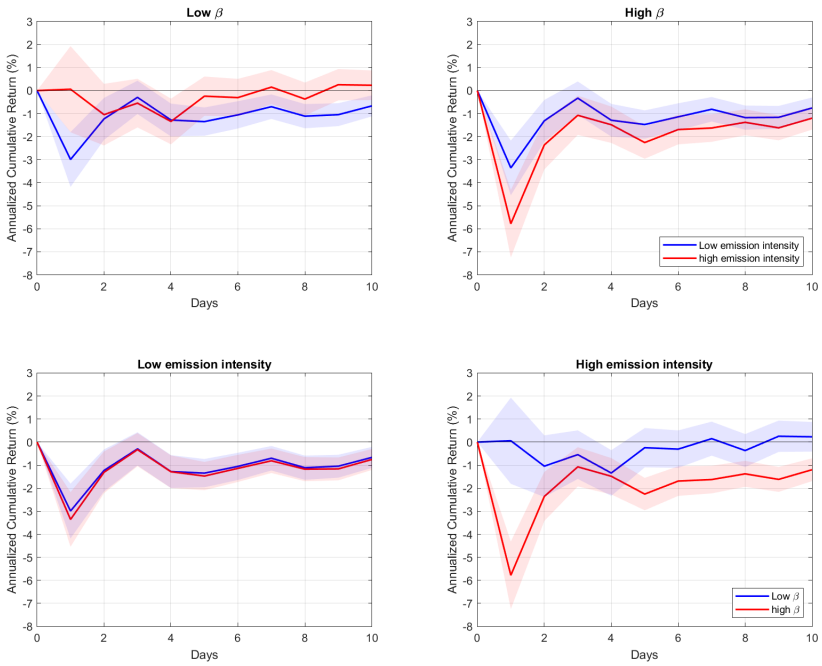


FIG. 10. LOCAL EQUITY RETURNS AND INNOVATIONS TO WORLD CAI

Notes: This figure shows the average cumulative return in equity returns after days with a top-15% positive spike in the global CAI. Returns are in local units (as opposed to USD) and in percentage. For more details, see the notes under figure 9.

firms in more exposed countries experience greater depreciation—is primarily driven by top-attention days dominated by concerns over physical risk.

Most importantly, our results are not solely driven by the exchange rate adjustment. As shown in figure 10, our results hold also when we focus on returns expressed in local currency.

Robustness. In Appendix B, we show that our results are robust across various methodological changes. Panel (a) in Figure B.10 uses GDP-weighted CAI, while Panel (b) employs Twitter Volume-weighted CAI. Both panels confirm the robustness of our findings as documented in Figure 9. Furthermore, Figure B.11 compares the

response of equity returns using thresholds of 10% and 20% to identify spikes in CAI, respectively. This figure documents that our results remain qualitatively unchanged regardless of the chosen threshold.

Figure B.12 provides supplementary analyses to validate our findings. In Panel (a) we cluster standard errors at the country$\times$industry$\times$date and firm levels, while in Panel (b) we use residual βs obtained by regressing our exposure coefficients on the University of Notre Dame's vulnerability index. These results corroborate our main conclusions.

4 Climate news shocks in general equilibrium.

The environment. The main equilibrium conditions of our model are derived in Appendix C. In what follows, we describe our economic environment and then derive the key predictions regarding trade and currencies. The model features two countries, home and foreign. Foreign variables are denoted by "$*$". Due to the symmetry of our environment, many of our equations are presented for the home country, with the implicit understanding that they apply to the foreign country as well. Time is discrete and we assume that there are only two periods denoted by the following three dates $t = 0, 1, 2$.

All shocks materialize at the end of the first period, i.e., at $t = 1$. Hence, at time $t = 0$ choices are made under uncertainty. At time $t = 2$, no additional shock materializes, or, equivalently, in the second period there is full resolution of uncertainty. Most importantly, all news received at time $t = 1$ affect the production frontier only at $t = 2$. Hence, from a time-1 perspective, these shocks represent pure news shocks.

In each country, the representative household has the following recursive preferences:

$$u_t = \begin{cases} (1-\beta)\log\left(C_t D_t^{-a}\right) + \frac{\beta}{1-\gamma}\log E_t\left[\exp\left\{u_{t+1}(1-\gamma)\right\}\right] & \gamma \neq 1 \\ (1-\beta)\log\left(C_t D_t^{-a}\right) + \beta E_t\left[u_{t+1}\right] & \gamma = 1 \end{cases}$$

When $\gamma = 1$, our preferences boil down to the case of log-expected utility. When $\gamma > 1$, instead, the households feature a preference for early resolution of uncertainty. Equivalently, households price news shocks, that is, their marginal utility immediately adjust with the arrival of news. Since we assume that there is full resolution of uncertainty at time $t = 1$, households are concerned about uncertainty about utility at time 1.

As in prior work, we assume that each agent consumes a bundle of two consumption goods:

$$C_t = X_t^{\lambda} Y_t^{(1-\lambda)}, \text{ and } \quad C_t^* = X_t^{*(1-\lambda)} Y_t^{*\lambda}, \quad t = 1, 2.$$

In what follows, we assume that X_t is the home-produced good, whereas Y_t is the foreign-produced good. The parameter $\lambda > 1/2$ is set so that there is home-bias in consumption. C_0 and C_0^* are both fixed paramters in this model.

D_t captures the damage caused by climate change and $0 < a < 1$ determines its impact on the household's utility. C_t denotes the consumption bundle at time t. We think of D_t as resulting from economic activity. Since in our model we abstract away from labor and capital is one-period ahead pre-determined, output at time 1 is pre-determined. As a result, D_0, D_0^*, D_1, and D_1^* are given in this setting. In contrast, at time $t = 2$, damages are endogenous and are modelled as follows:

$$D_2 = e^{bg}\left(e^{\theta} G / I_{g,1}\right)^{\lambda_g}\left(e^{-\theta} G^* / I_{g,1}^*\right)^{1-\lambda_g}, \quad D_2^* = e^{g}\left(e^{-\theta} G^* / I_{g,1}^*\right)^{\lambda_g}\left(e^{\theta} G / I_{g,1}\right)^{1-\lambda_g}.$$

The term e^g captures a global climate news shock with $g \sim N(0, \sigma_g^2)$. The exposure of the foreign country to this shock is normalized to 1, whereas b captures the exposure of the home country. When $b > 1$, the home country is more exposed than the foreign one. Therefore, $b \neq 1$ captures heterogenous exposure to a common climate shock. The parameter λ_g determines the relevance of home-originated emissions relative to foreign-originated emissions. When $\lambda_g = 0.5$, agents are equally concerned about domestic and foreign emissions. When $\lambda_g > 0.5$, local emissions produce stronger damages.

At time $t = 2$, output is assumed to be equal to $e^{\theta}G$ and $e^{-\theta}G^*$ in the home and foreign country, respectively. The term e^{θ} determines a local productivity shock, with $\theta \sim i.i.d.N(0, \sigma_\theta^2)$. When $\theta > 0$, the home country is $2\theta\%$ more productive than the foreign country. G and G^* are bundles of time-1 local and foreign investments in the home- and foreign-country, respectively:

$$G = I_{x,1}^{\lambda_I} I_{x,1}^{*1-\lambda_I}, \text{ and } G^* = I_{y,1}^{1-\lambda_I} I_{y,1}^{*\lambda_I},$$

Note that when $\lambda_I = \lambda$, the consumption bundle is identical to the investment bundle in each country. Given these assumptions, the damage in each country is a combination of economic activity (output) both at home and abroad.

Finally, $I_{g,1}$ and $I_{g,1}^*$ represent green investments in the home and foreign country, respectively. These components capture the ability of reducing the impact of output on climate by investing in new greener technologies.

At time $t = 1$, output is predetermined and fixed to 1 for simplicity. The implied

resource constraints in the economy are standard,

$$1 = X_1 + X_1^* + I_{x,1} + I_{y,1} + I_{g,1}, \qquad 1 = Y_1 + Y_1^* + I_{y,1}^* + I_{x,1}^* + I_{g,1}^*,$$

and account for both international flows of consumption and investment goods. At time $t = 2$, there is no incentive to further invest in capital as we are focusing on a 2-period model. Hence time-2 output is solely used to support international consumption:

$$e^{\theta} G = X_2 + X_2^*, \qquad e^{-\theta} G^* = Y_2 + Y_2^*.$$

Returns. In this economy, we define the returns to both brown and green capital across periods. Between time-1 and time-2, all returns equal the risk-free rate because there is full resolution of uncertainty at time-1. Between time-0 and time-1, however, returns are random as they depend on stochastic fundamentals.

Let $r_{x,1} - r_{g,1}$ represent the excess return of a zero-dollar investment strategy that is long in home country brown capital and short in its green capital. In the Appendix, we demonstrate that the following equation holds:

$$r_{x,1} - r_{g,1} = constant + \lambda^s_{r_x - r_b} \lambda^{\theta}_s \theta + \lambda^s_{r_x - r_b} \lambda^g_s g, \tag{6}$$

where the terms denoted by λ^*_* are composite exposure coefficients whose signs can be analytically determined. In Appendix C, we address the planner's problem associated with this setting. Additionally, we explore an environment where emission externalities have been corrected and the economy is at its first-best. In this setting, we derive several testable hypotheses that we describe below.

Additional Testable hypotheses. In Appendix C, we prove the following two propositions.

Proposition 1. *If $b > 1$, the brown-minus-green investment return in the home country depreciates when there is a positive global climate news shock g. In addition, the effect is stronger with a higher b.*

In the appendix, we show that the coefficient $\lambda^s_{r_x - r_b} < 0$, and $\lambda^g_s > 0$ when b is greater than 1. This means that in countries with relatively high exposure, climate shocks have a greater impact on brown stocks. Additionally, $\lambda^g_s > 0$ increases with the level of country exposure, denoted by b. This finding aligns with our empirical approach where we consider the interaction between firm-level emissions and country exposure (equations (4) and (5)).

Proposition 2. *Let $\gamma > 1$, when $b > 1$ ($b < 1$), a global climate news shock $g > 0$ causes an appreciation of home (foreign) real exchange rate.*

Proposition 2 confirms what we have derived in the previous section when adopting a no-arbitrage approach. Namely, adverse global news shocks to climate cause an appreciation of currencies associated to countries relatively more exposed to these news.

Proposition 3. *When $b > 1$, a global climate news shock $g > 0$ increases the relative pseudo Pareto weight of the home country, S_1, and it decreases the net exports of consumption and investment goods, $\frac{NX_1^C}{X_1}$ and $\frac{NX_1^I}{I_x}$.*

In order to better explain proposition 3, we find it appropriate to focus on the equilibrium the net exports of consumption goods,

$$\frac{NX_1^C}{X_1} - \frac{NX_1^{C*}}{Y_1^*} = \beta_\theta^{NX} \cdot 2\theta + \beta_g^{NX}(b-1)g.$$

In the appendix, we prove that under the assumptions detailed in our propositions the coefficients in front of the three fundamental shocks have the following structure and signs:

$$\begin{aligned}\beta_{\theta}^{NX} &= -\frac{1}{2}\frac{1-\lambda}{\lambda}(e^{\bar{s}_1}-e^{-\bar{s}_1})\lambda_s^{\theta}>0\\ \beta_{g}^{NX} &= -\frac{1}{2}\frac{1-\lambda}{\lambda}(e^{\bar{s}_1}-e^{-\bar{s}_1})\frac{\lambda_s^{g}}{b-1}<0.\end{aligned}$$

Since similar results hold for net exports of investment goods, the sign of these coefficients apply also to the difference of the total net exports. For the home country, a positive productivity shock generates an outflow of resources to the foreign country. In contrast, an adverse shock to global climate generates an outflow only if the home country has a moderate exposure to it, $b<1$.

Empirical tests for international trade. In the data, we are interested in estimating the following system of equations:

$$\Delta CAI_{i,t} = \beta_i \cdot \overline{\Delta CAI}_t + u_{i,t} \tag{7}$$

$$\begin{aligned}\Delta\left(\frac{NX_{i,t}}{GDP_{i,t}}\right)-\Delta\left(\frac{NX_{j,t}}{GDP_{j,t}}\right) &= \Gamma\cdot(\beta_i-\beta_j)\,\overline{\Delta CAI}_t+...\\ &\quad +\theta'\cdot(control_{i,t}-control_{j,t})+\epsilon_{ij,t},\end{aligned} \tag{8}$$

where $\frac{NX_{i,t}}{GDP_{i,t}}$ is the net export over GDP of country i at time t. We add the first difference to make sure that all variables are stationary. $\Delta CAI_{i,t}$ denotes the growth rate of the climate attention index for country i and quarter t, $\overline{\Delta CAI}_t$ is the cross-sectional

average of ΔCAI_t at date t, i.e., the global CAI index.[11] The term $control$ is a vector of control variables including the change in the industrial production index (ΔIPI), to control for country-specific productivity shocks, and the share of Twitter volume on days when the CAI is at the bottom 5%, to control for other events that affect Twitter activities. In the appendix, we consider a more general version of our model which features also local climate news shocks with volatility σ_z. In main text, we abstract away from local shocks by setting $\sigma_z = 0$ because in our international setting global shocks feature a prominent role.

We provide results based on the cases in which $\overline{\Delta CAI}_t$ is constructed in one of three ways: (i) by equally weighting all countries, (ii) by weighting each country proportionally to its share of global GDP, and (iii) by weighting each country proportionally to its share of Twitter volumes.

Simple OLS on both equations will produce incorrect inference for the coefficient Γ, because the β coefficients in equation (8) are themselves estimated from equation (7). We address this econometric issue by estimating the system via GMM with a pre-determined weighting matrix. Specifically, the set of moment conditions is

$$g_T(\beta, \gamma, \theta) = E_T \begin{bmatrix} u_{i,t}\overline{\Delta CAI}_t \\ \epsilon_{ij,t}\left(\beta_i - \beta_j\right)\overline{\Delta CAI}_t \\ \epsilon_{ij,t}\left(control_{i,t} - control_{j,t}\right) \end{bmatrix} = E_T \begin{bmatrix} g_1(\beta) \\ g_2(\beta, \Gamma, \theta) \end{bmatrix}$$

where $g_1(\beta)$ is the vector of orthogonality conditions associated to equation (7) for each country i, and $g_2(\beta, \Gamma, \theta)$ stacks the three orthogonality conditions associated to equation (8) for each country pair $\{i, j\}$. The first block g_1 pins down β, and the second

[11] In order to eliminate the effect of the Covid-19 and the beginning of the war in Ukraine, we have regressed $\Delta CAI_{i,t}$ on two dummies of 2020Q2 and 2022Q1 for each country, and obtain the residual for our analysis.

block g_2 pins down the remaining coefficients Γ, θ. Given two control variables, if we have N countries in our sample, the number of moments will be $N + 2N \times (N-1)$, and the number of parameters is $N + 4$. This is an over-identified GMM problem for $N > 2$.

Next, we follow Cochrane (2009) and estimate the following linear combination of the moment conditions:

$$a_T g_T = 0$$

where

$$a_T = \begin{bmatrix} I_N & 0 \\ 0 & \frac{\partial g_2(\beta,\gamma,\theta)}{\partial[\gamma,\theta]} W \end{bmatrix}$$

with I_N and W being identity matrices of size N and $2N \times (N-1)$, respectively. Weighting the block of orthogonality conditions of equation 7 with an identity matrix ensures that the estimated vector of βs coincides with OLS estimates. The set of moments conditions in g_2 is instead efficiently estimated. Denote by $b = [\beta, \gamma, \theta]'$ the vector of all parameters. The asymptotic distribution of b is given by

$$\sqrt{T}(\hat{b} - b) \sim N\left(0, (ad)^{-1} a S a' (ad)'^{-1}\right)$$

where $a = \lim_{T\to\infty} a_T$, $d = \frac{\partial g_t}{\partial b}$ is the gradient, and S is the spectral density matrix estimated using the residuals.

Given our interest on the role of global climate news shocks on the dynamics of international trade, we focus on the estimated parameter Γ in equation (8). According to our model, this coefficient should be negative. We estimate the parameters of interest using an expanding window to show whether the estimated coefficient is stable over different sample periods. Specifically, we fix our starting period at 2015:Q1

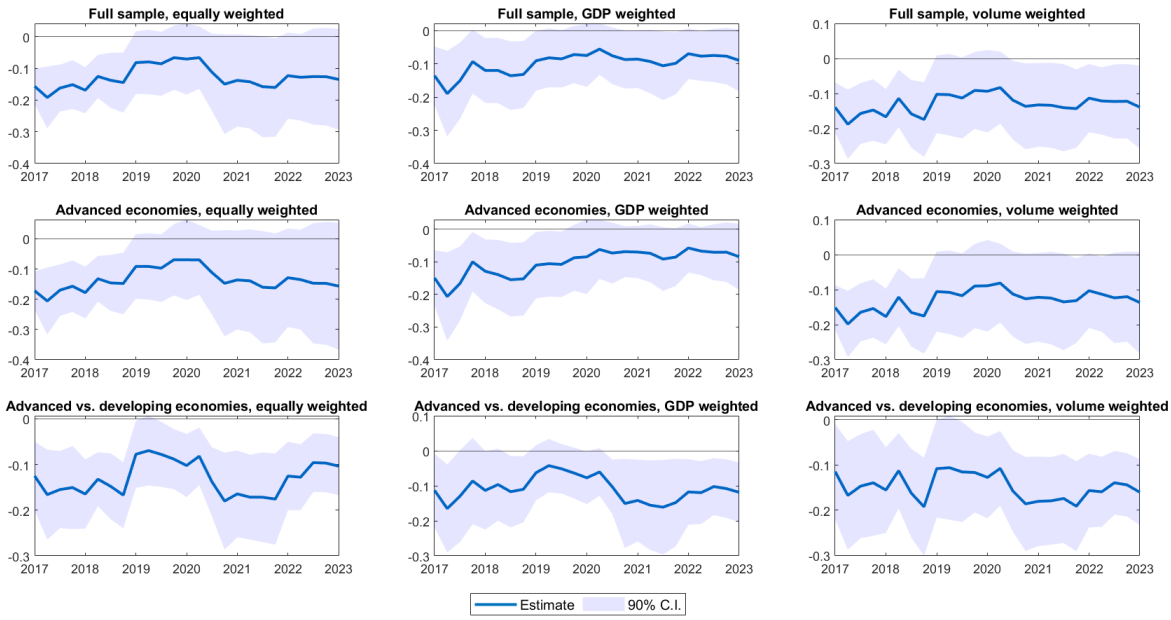


FIG. 11. GMM ESTIMATION OF Γ.

Notes: The figure shows estimates of Γ (defined in equation (8)) using expanding time windows. Each window starts in 2015:Q1 and ends on the date reported on the x-axis. The parameter Γ is estimated using the GMM described in section 4. Panels in different columns refer to results obtained from different ways to aggregate country-level CAI indices in order to form a global component. Panels in different rows refer to results obtained from different groups of country-pairs. Advanced economies are defined according to the IMF. Standard errors are HAC-adjusted. The shaded areas present the 90% confidence interval.

(where our sample begins), and expand the end of sample from 2016:Q4 to 2022:Q4. The estimated Γ coefficient along with its 90% confidence interval are presented in figure 11.

Our estimates support the prediction of our model, as they suggest that an adverse global climate shock produces an outflow of resources away from countries with a lower exposure. This result is confirmed across different ways to aggregate our country-level CAI in order to form a global index. In addition, our result is driven mainly by country pairs in which there is at least one developed economy. This is broadly consistent with the spirit of our model since we assume that risk sharing is implemented with frictionless trade.

5 Concluding Remarks

Our research significantly contributes to our understanding of the impact of global climate attention on economic and financial outcomes. The availability of high frequency data is particularly valuable as it enables a more direct analysis of how climate news shocks reverberate throughout global financial markets and influence currencies on a global scale. The establishment of a clear connection between climate attention shocks and bilateral trade among nations represents a noteworthy advancement for both the macro-finance literature and policymakers.

Moreover, the economic model we introduce, along with the climate attention index we propose, open up various avenues for future research. For instance, our economic theory implies that heightened global news attention to climate issues may influence decisions regarding investments in green technology. Furthermore, the climate attention index we have developed can be leveraged to explore the relationship between climate-related news and returns on a wide range of assets above and beyond stocks, both within individual countries and across international borders. These potential research directions hold promise for gaining deeper insights into the complex interplay between climate awareness and economic and financial dynamics.

Establishing a connection between attention to climate news and currency movements is of paramount importance in the current global landscape. As climate change becomes an increasingly pressing concern, understanding how shifts in climate attention impact financial markets and trade can inform both economic policies and investment strategies. It provides a valuable tool for policymakers to anticipate and respond to economic implications of climate-related events and offers investors insights into the potential risks and opportunities associated with climate awareness.

By shedding light on these intricate connections, our research serves not only the academic community but also contributes to the broader efforts to address the multi-faceted challenges posed by climate change on a global scale.

References

Acharya, V. V., T. Johnson, S. Sundaresan, and T. Tomunen. Is physical climate risk priced? evidence from regional variation in exposure to heat stress. Technical Report w30445 National Bureau of Economic Research 2022 https://www.nber.org/papers/w30445.

Alekseev, G., S. Giglio, Q. Maingi, J. Selgrad, and J. Stroebel. A quantity-based approach to constructing climate risk hedge portfolios. Technical report National Bureau of Economic Research 2021 https://www.nber.org/papers/w30703.

Baker, S. R., N. Bloom, and S. J. Davis. 2016. Measuring economic policy uncertainty*. The Quarterly Journal of Economics 131(4):1593.

Bansal, R., D. Kiku, and M. Ochoa. Climate change risk. Technical report Federal Reserve Bank of San Francisco 2019 https://www.frbsf.org/economic-research/events/2019/november/economics-of-climate-change/files/Paper-5-2019-11-8-Kiku-1PM-1st-paper.pdf.

Barbieri, F., L. Espinosa Anke, and J. Camacho-Collados. XLM-T: Multilingual language models in Twitter for sentiment analysis and beyond. In Proceedings of the Thirteenth Language Resources and Evaluation Conference. European Language Resources Association 06 2022.

Bolton, P., and M. Kacperczyk. 2021. Do investors care about carbon risk? Journal of Financial Economics 142(2):517–549. doi: 10.1016/j.jfineco.2021.05.008.

Bolton, P., and M. Kacperczyk. 2023. Global pricing of carbon-transition risk. Journal of Finance 78(6):3677–3754. doi: 10.1111/jofi.13272.

Bolton, P., M. T. Kacperczyk, and M. Wiedemann. The co2 question: Technical progress and the climate crisis. Technical report Working Paper 2023 https://ssrn.com/abstract=4212567.

Cochrane, J. Asset pricing: Revised edition. Princeton university press 2009.

Colacito, R., M. Croce, S. Ho, and P. Howard. November 2018. Bkk the ez way: International long-run growth news and capital flows. American Economic Review 108(11):3416–49.

Colacito, R., B. Hoffmann, and T. Phan. 2019. Temperature and growth: A panel analysis of the united states. Journal of Money, Credit and Banking 51(2-3):313–368. doi: https://doi.org/10.1111/jmcb.12574.

Della Corte, P., L. Sarno, and I. Tsiakas. 2009. An Economic Evaluation of Empirical Exchange Rate Models. Review of Financial Studies 22(9):2491–530.

Della Corte, P., L. Sarno, and I. Tsiakas. 2011. Spot and forward volatility in foreign exchange. Journal of Financial Economics 100(3):496 – 513.

Della Corte, P., T. Ramadorai, and L. Sarno. 2016. Volatility risk premia and exchange rate predictability. Journal of Financial Economics 120(1):21 – 40. ISSN 0304-405X.

Engle, R. F., S. Giglio, B. Kelly, H. Lee, and J. Stroebel. 2020. Hedging Climate Change News. The Review of Financial Studies 33(3).

Giglio, S., B. Kelly, and J. Stroebel. 2021a. Climate finance. Annual Review of Financial Economics 13:15–36. doi: 10.1146/annurev-financial-102620-103311.

Giglio, S., M. Maggiori, K. Rao, J. Stroebel, and A. Weber. 2021b. Climate change and long-run discount rates: Evidence from real estate. The Review of Financial Studies 34(8):3527–3571. doi: 10.1093/rfs/hhab032.

Giglio, S., T. Kuchler, J. Stroebel, and X. Zeng. Biodiversity risk. Technical Report w31137 National Bureau of Economic Research 2023 https://www.nber.org/papers/w31137.

Grootendorst, M. 2022. Bertopic: Neural topic modeling with a class-based tf-idf procedure. arXiv preprint arXiv:2203.05794.

Hassan, T. 2013. Country size, currency unions, and international asset returns. The Journal of Finance 68:2269–308.

Hassan, T., T. Mertens, and T. Zhang. 2015. Currency manipulation. Working Paper.

Hassan, T. A., T. M. Mertens, and T. Zhang. 2016. Not so disconnected: Exchange rates and the capital stock. Journal of International Economics 99:S43–S57.

Hassan, T. A., S. Hollander, L. Van Lent, and A. Tahoun. 2019. Firm-level political risk: Measurement and effects. The Quarterly Journal of Economics 134(4):2135–2202.

Hassan, T. A., J. Schreger, M. Schwedeler, and A. Tahoun. 2023. Sources and Transmission of Country Risk. The Review of Economic Studies. ISSN 0034-6527.

Hijioka, Y., E. Lin, J. J. Pereira, R. T. Corlett, X. Cui, G. Insarov, R. Lasco, E. Lindgren, A. Surjan, E. M. Aizen et al. 2014. Ipcc fifth assessment report: Chapter 24 asia. Intergovernmental Panel on Climate Change pages 1327–1370.

Hsu, P.-h., K. Li, and C.-y. Tsou. 2023. The pollution premium. The Journal of Finance 78(3): 1343–1392.

Javadi, S., A.-A. Masum, M. Aram, and R. P. Rao. 2023. Climate change and corporate cash holdings: Global evidence. Financial Management 52(2):253–295.

Kashyap, A., N. Kovrijnykh, and A. Pavlova. 2024. Designing esg benchmarks. Working paper.

Lee, S. O., N. C. Mark, J. Nauerz, J. Rawls, and Z. Wei. 2022. Global temperature shocks and real exchange rates. Journal of Climate Finance 1:100004.

Leombroni, M., A. Vedolin, G. Venter, and P. Whelan. 2021. Central bank communication and the yield curve. Journal of Financial Economics 141(3). ISSN 0304-405X.

Lustig, H., N. Roussanov, and A. Verdelhan. 2011. Common risk factors in currency markets. Review of Financial Studies 24:3731–77.

Lustig, H., N. Roussanov, and A. Verdelhan. 2014. Countercyclical currency risk premia. Journal of Financial Economics 111(3):527–553.

Mueller, P., A. Stathopoulos, and A. Vedolin. 2017. International correlation risk. Journal of Financial Economics.

Pástor, L., R. F. Stambaugh, and L. A. Taylor. 2021. Sustainable investing in equilibrium. Journal of Financial Economics 142(2):550–571. doi: 10.1016/j.jfineco.2020.12.011.

Pástor, L., R. F. Stambaugh, and L. A. Taylor. 2022. Dissecting green returns. Journal of Financial Economics 146(2):403–424. doi: 10.1016/j.jfineco.2022.07.007.

Pavlova, A., and R. Rigobon. 2007. Asset prices and exchange rates. Review of Financial Studies 20:1139–1181.

Pavlova, A., and R. Rigobon. 2010. An asset-pricing view of external adjustment. Journal of International Economics 80:144–156.

Pavlova, A., and R. Rigobon. 2013. International macro-finance. Handbook of Safeguarding Global Financial Stability: Political, Social, Cultural, and Economic Theories and Models 2: 169–176.

Pedersen, L. H., S. Fitzgibbons, and L. Pomorski. 2021. Responsible investing: The esg-efficient frontier. Journal of Financial Economics 142(2):572–597. doi: 10.1016/j.jfineco.2020.11.001.

Pigato, M. A., and F. E. Stewart. 2020. Climate change in apec: Assessing risks, preparing financial markets, and mobilizing institutional investors. World Bank Report.

Reimers, N., and I. Gurevych. Sentence-bert: Sentence embeddings using siamese bert-networks. In Proceedings of the 2019 Conference on Empirical Methods in Natural Language Processing. Association for Computational Linguistics 11 2019.

Sandulescu, M., F. Trojani, and A. Vedolin. 2020. Model-free international stochastic discount factors. Journal of Finance. forthcoming.

Sautner, Z., L. Van Lent, G. Vilkov, and R. Zhang. 2023. Firm-Level Climate Change Exposure. Journal of Finance.

Starks, L. T. 2023. Presidential address: Sustainable finance and esg issues – value versus values. Journal of Finance 78:1837–1872. doi: 10.1111/jofi.13255.

Sun, Y., X. Zhang, Y. Ding, D. Chen, D. Qin, and P. Zhai. 2022. Understanding human influence on climate change in china. National science review 9(3):nwab113.

Yang, B. 2021. Explaining greenium in a macro-finance integrated assessment model. Working paper. Available at SSRN: https://ssrn.com/abstract=3854432 or http://dx.doi.org/10.2139/ssrn.3854432.

Zviadadze, I. 2017. Term structure of consumption risk premia in the cross section of currency returns. Journal of Finance.

Appendix A. Data collection

TABLE A.1: Newspaper Twitter Handles by Country

Country	Newspaper name	Twitter handle	Language
Argentina	Clarín	clarincom	Spanish
	Diario Crónica	cronica	
	Infobae	infobae	
	La Nación	LANACION	
Australia	The Australian	australian	English
	The Daily Telegraph	dailytelegraph	
	The Australian Financial Review	FinancialReview	
	The Age	theage	
Brazil	Estadão	Estadao	Portuguese
	Folha de S.Paulo	folha	
	GauchaZH	GauchaZH	
	Jornal O Globo	JornalOGlobo	
Canada	The Globe and Mail	globeandmail	English
	Montreal Gazette	mtlgazette	
	Ottawa Citizen	OttawaCitizen	
	Toronto Star	TorontoStar	
	The Vancouver Sun	VancouverSun	
Switzerland	20 Minuten	20min	German
	24 heures	24heuresch	
	Le Temps	LeTemps	French
	Neue Zürcher Zeitung	NZZ	
Chile	El Mercurio	ElMercurio_cl	Spanish
	El Mostrador	elmostrador	
	La Tercera	latercera	
China	China Daily	ChinaDaily	English
	People's Daily China	PDChina	
	China Xinhua News	XHNews	
Colombia	El Colombiano	elcolombiano	Spanish
	El Espectador	elespectador	
	El Heraldo Colombia	elheraldoco	
Germany	BILD	BILD	German
	Frankfurter Allgemeine	faznet	
	Handelsblatt	handelsblatt	
	ZEIT ONLINE	zeitonline	
Spain	ABC	abc_es	Spanish
	El País	el_pais	
	El Mundo	elmundoes	
	La Vanguardia	LaVanguardia	
France	Le Figaro	Le_Figaro	French
	Le Parisien	le_Parisien	
	Le Monde	lemondefr	

Country	Newspaper name	Twitter handle	Language
	Libération	libe	
China (Hong Kong)	Hong Kong Free Press RTHK News SCMP News	HongKongFP rthk_enews SCMPNews	English
India	Economic Times Hindustan Times The Hindu Times of India	EconomicTimes htTweets the_hindu timesofindia	English
Italy	Corriere della Sera Repubblica Il Sole 24 ORE	Corriere repubblica sole24ore	Italian
Japan	Asahi Shimbun AJW The Japan Times Japan Today The Japan News	AJWasahi japantimes JapanToday The_Japan_News	English
Korea	The Korea JoongAng Daily The Korea Times The Korea Herald Yonhap News	JoongAngDaily koreatimescokr TheKoreaHerald YonhapNews	English
Mexico	El Universal La Jornada Milenio Reforma	El_Universal_Mx lajornadaonline Milenio Reforma	Spanish
Norway	Aftenposten Dagbladet VG	Aftenposten dagbladet vgnett	Norwegian
New Zealand	Dominion Post ODT - Otago Daily Times The Press Newsroom	DomPost odtnews PressNewsroom	English
Portugal	Correio da Manhã Expresso Jornal de Notícias	cmjornal expresso JornalNoticias	Portuguese
Saudi Arabia	Al Jazirah Alwatan OKAZ	al_jazirah AlwatanSA OKAZ_online	Arabic
Sweden	Dagens Nyheter Goteborgs Posten Svenska Dagbladet Sydsvenskan	dagensnyheter GoteborgsPosten SvD sydsvenskan	Swedish
United Kingdom	BBC News Financial Times The Guardian The Times and The Sunday Times	BBCNews FinancialTimes guardiannews thetimes	English
United States	Boston Globe	BostonGlobe	English

Country	Newspaper name	Twitter handle	Language
	Chicago Tribune	chicagotribune	
	Dallas News	dallasnews	
	Houston Chronicle	HoustonChron	
	LA Times	latimes	
	Miami Herald	MiamiHerald	
	NY Times	nytimes	
	SF Chronicle	sfchronicle	
	USA Today	USATODAY	
	Washinton Post	washingtonpost	
	Wall Street Journal	WSJ	
South Africa	Daily Sun	dailysunsa	English
	Sunday Times	SundayTimesZA	
	Times Live	TimesLIVE	

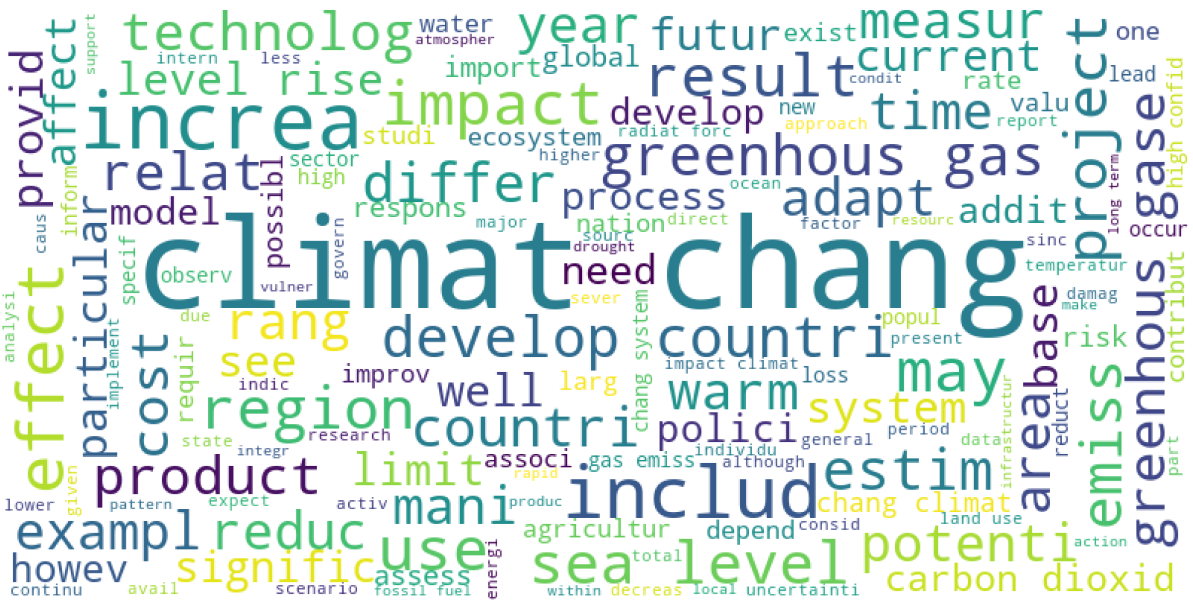


FIG. A.1. WORD CLOUD FOR THE PRE-PROCESSED CORPUS

Notes: This figure shows the cloud of the word roots of authoritative texts used in the construction of the Climate Attention Index. See Engle et al. (2020). Our preprocess: (1) removes any special characters and/or numbers, (2) removes stop words (e.g, "and" "or"), (3) stems each word (using the Snowball algorithm), and (4) keeps only words with more than two characters. We translated this corpus to different languages to build an index for non-English speaking countries.

TABLE A.2. AI-GENERATED SENTENCES

	Physical Risk	Transition Risk
1	Hurricanes are becoming more intense	New carbon taxes increase energy costs
2	Rising sea levels threaten coastal cities	Governments are enforcing stricter emission limits
3	Wildfires are spreading faster each year	Climate policies impact fossil fuel investments
4	Floods are more frequent in urban areas	Carbon pricing is affecting industry competitiveness
5	Droughts are lasting longer worldwide	Environmental regulations are tightening worldwide
6	Heatwaves are breaking records globally	Firms must comply with stricter sustainability laws
7	Cyclones are forming earlier than expected	Carbon offsets are becoming a mandatory requirement
8	Tornadoes are appearing in new regions	Subsidies for renewable energy are rising
9	Storm surges endanger coastal communities	Stricter reporting rules affect corporate disclosures
10	Melting glaciers contribute to rising seas	Regulatory risks impact financial markets
11	Arctic ice is melting at record speeds	Fossil fuel demand is declining
12	Permafrost is thawing, releasing methane	Renewable energy adoption is accelerating
13	Global temperatures are steadily increasing	Investors are divesting from coal industries
14	Extreme cold events are less frequent	Gas prices fluctuate due to energy transitions
15	Ocean temperatures are rising rapidly	Green bonds are reshaping capital markets
16	Coral reefs are dying due to warming seas	The electric vehicle market is expanding rapidly
17	Changing seasons affect crop production	Oil companies face increasing financial pressure
18	More frequent heatwaves strain electricity grids	Hydrogen energy is gaining policy support
19	Polar vortex disruptions cause unusual cold	Nuclear power investments are rising
20	Snowfall patterns are shifting globally	Battery storage is critical for renewable energy growth
21	Rivers are drying up due to prolonged droughts	Energy efficiency technologies are reshaping industries
22	Flash floods destroy homes and roads	Carbon capture projects are scaling up
23	Drinking water sources are shrinking	Solar power efficiency is improving rapidly
24	Groundwater levels are depleting	Wind farms are replacing coal plants
25	Heavy rainfall increases landslide risks	Smart grids are enabling decentralized energy systems
26	Freshwater lakes are shrinking worldwide	Climate-friendly materials are replacing traditional ones
27	Ice sheets are collapsing faster than expected	Green hydrogen is becoming more viable
28	Saltwater intrusion threatens freshwater supplies	Electrification of transportation is accelerating
29	Dams are failing under extreme weather	Sustainable agriculture technologies are emerging
30	Reservoirs are running dry in many regions	Circular economy practices are gaining traction
31	Desertification is expanding in dry regions	Lawsuits against polluting companies are increasing
32	Livestock suffers from water shortages	Investors are demanding climate risk disclosures
33	Pests spread as temperatures rise	Regulators require firms to report climate risks
34	Changing climates affect coffee production	Non-compliance with emissions laws leads to penalties
35	Soil erosion worsens with heavy rain	Litigation risks threaten fossil fuel companies
36	Crop yields are declining due to heat stress	Banks must assess climate risks in lending portfolios
37	Unpredictable rainfall disrupts farming	Corporate climate pledges face legal scrutiny
38	Fisheries collapse due to warming oceans	Greenwashing claims lead to reputational damage
39	Extreme weather damages food supply chains	Disclosure failures result in investor lawsuits
40	More frequent frost events harm fruit crops	Companies face pressure to adopt net-zero targets
41	Roads crack under extreme heat	Job losses in fossil fuel industries are rising
42	Floods overwhelm drainage systems	Green jobs are reshaping the labor market
43	Airports close due to extreme weather	Energy prices are volatile due to policy shifts
44	Power outages increase with heatwaves	Consumer preferences are shifting toward sustainability
45	Rising insurance costs strain homeowners	Supply chains are adapting to climate policies
46	Heat damages rail tracks and highways	Financial institutions are reassessing climate risks
47	Coastal erosion threatens real estate	Insurance premiums rise due to climate-related policies
48	Ports are closing due to severe storms	Carbon-intensive industries face declining revenues
49	Cold snaps increase energy demand	Developing economies struggle with climate transition costs
50	Business disruptions rise with climate events	Global trade patterns are shifting due to decarbonization

Notes: This table shows sentences randomly generated by ChatGPT about climate physical and transition risk.

Appendix B. Additional Empirical Results

Significance of climate attention βs. Figure B.1 depicts the values of the t-stat used to test the following null assumption $H_0 : \beta_i - \beta_j = 0, i \neq j$ for all possible country pairs in our dataset. The test is based on a joint estimation of equation (2) for each possible pair of country i and j. Dark colors refer to values of the t-stat with an associated confidence level smaller than 10%. We depict the country-pair test results only in the bottom portion of the figure because the upper portion is symmetric.

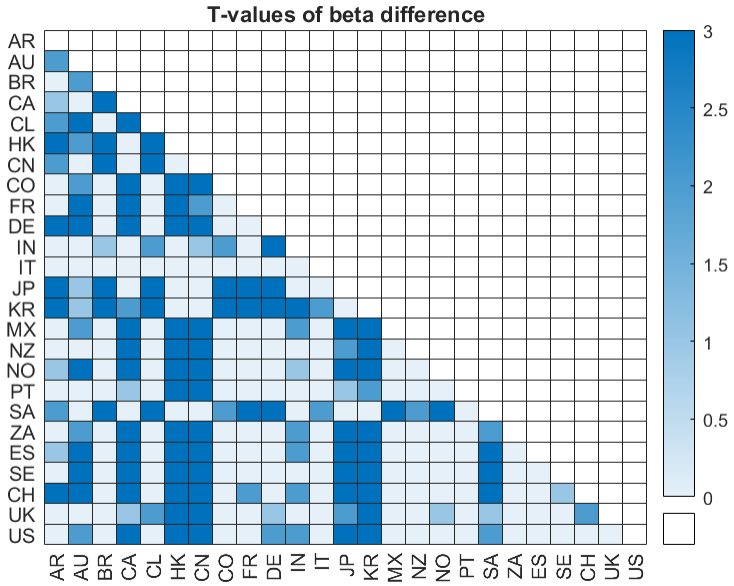
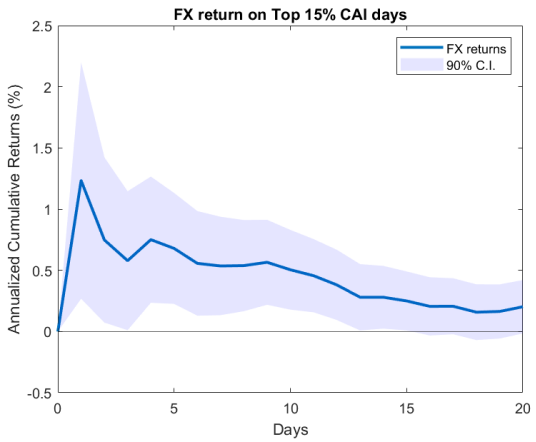


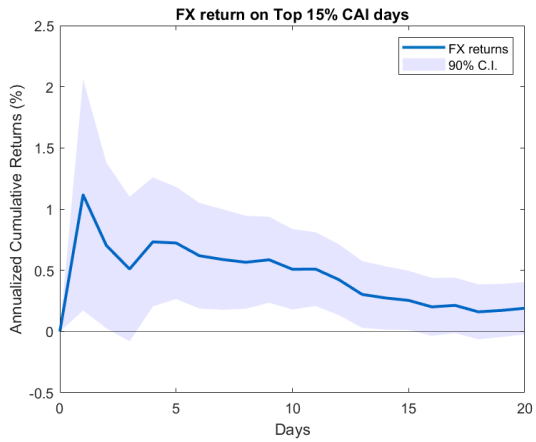
FIG. B.1. HETEROGENEOUS EXPOSURES ACROSS COUNTRY PAIRS

Notes: This figure shows the values of the t-stat used to test the following null assumption $H_0 : \beta_i - \beta_j = 0, i \neq j$ for all possible country pairs in our dataset. The test is based on a joint estimation of equation (2) for each possible pair of country i and j. Dark colors refer to values of the t-stat with an associated confidence level smaller than 10%. We depict the country-pair test results only in the bottom portion of the figure because the upper portion is symmetric.

Robustness of FX response. Figures B.2(a)-B.2(b) are constructed as figure 7 reported in main text, except that we compute our global CAI by weighting our countries by their GDP and tweets volume, respectively.



B.2(a) GDP-Weighted



B.2(b) Volume-Weighted

FIG. B.2. FX AND WORLD CAI: THE ROLE OF THE WEIGHTING SCHEME.

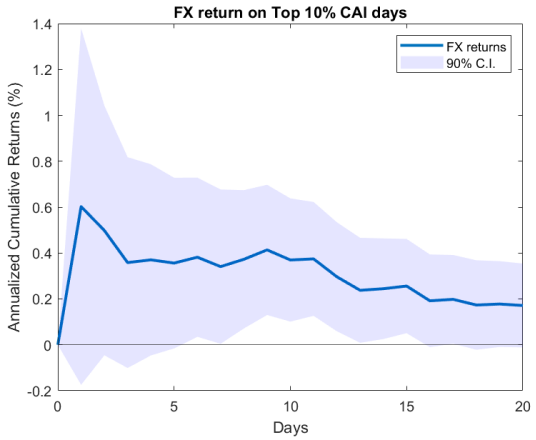
Notes: average cumulative return in exchange rates after days with a positive spike in the global CAI. Panel A is constructed as figure 7 except that country exposures are obtained by regressing country-level CAI on the GDP-weighted global CAI. Panel B is constructed as figure 7 except that country exposures are obtained by regressing country-level CAI on the Twitter Volume-weighted global CAI.

In figures B.3(a)-B.3(b) we consider top-10% and top-20% days, respectively. Our results are not sensitive to the percentile that we choose.

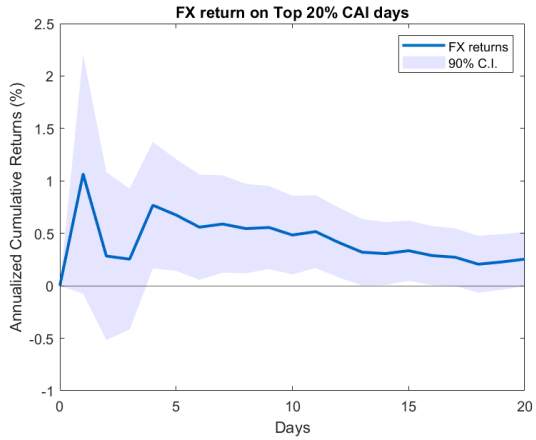
Figures B.4(a)-B.4(b) confirm that our results are not sensitive to the choice of the significance level that we use in order to select country-pairs with different exposure coefficients. Our results apply regardless of whether we include all country pairs (including those with modest heterogeneity in beta) or just those with a more pronounced degree of heterogeneity (5% confidence level).

Figure B.5(a) shows that our results are confirmed also when we aggregate five Euro Area countries in our datatset (DE, FR, IT, PT, ES) in just one entity with one currency. Most importantly, figure B.5(b) confirms that our results are not driven by vulnerability, but rather by the unique information content of our estimated esposure coefficients.

Figure B.6(a) confirms our main findings when using exposures estimated at the monthly frequency. Figure B.6(b) is constructed as figure 7 in main text, but it uses weekly observa-



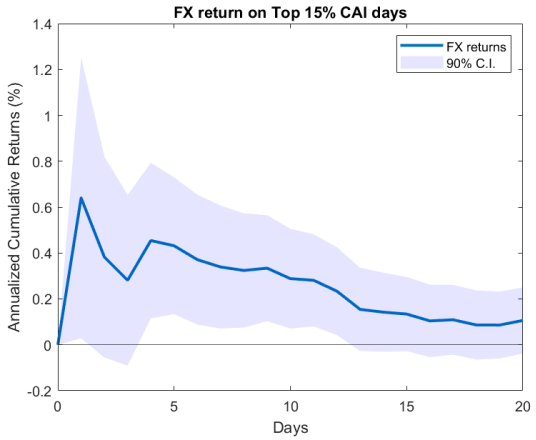
B.3(a) Top 10% Days



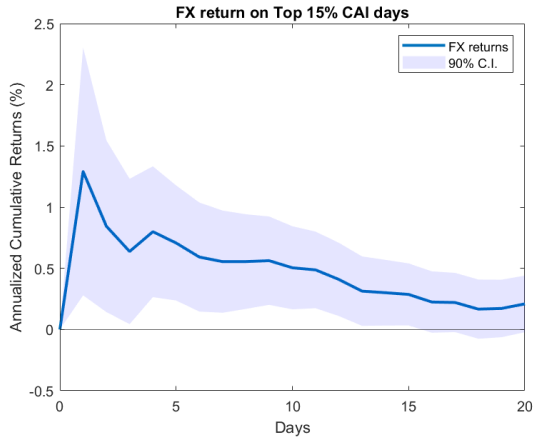
B.3(b) Top 20% Days

FIG. B.3. FX AND WORLD CAI: THE ROLE OF THE THRESHOLD.

Notes: average cumulative return in exchange rates around days with a positive spike in the global CAI. Panel A selects the top CAI days according to a top-10% threshold, while Panel B selects the top CAI days according to a top-20% threshold. For more details, see the notes under figure 7.



B.4(a) All Country Pairs

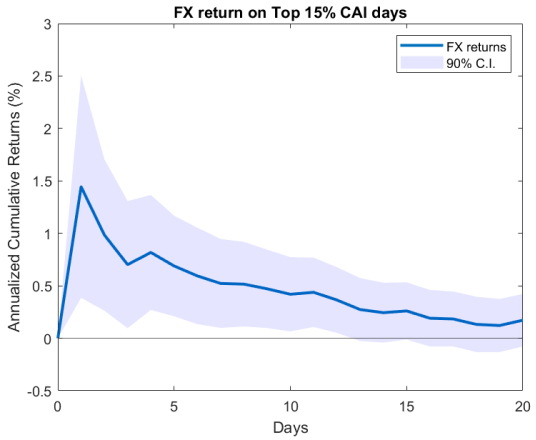


B.4(b) β Different at 5%

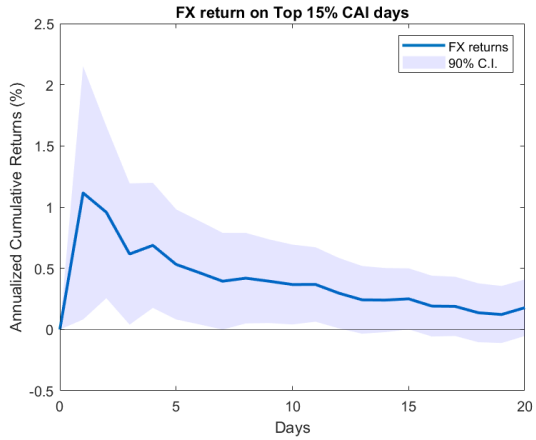
FIG. B.4. FX AND WORLD CAI: THE ROLE OF β.

Notes: average cumulative return in FX rates after days with a positive spike in global CAI. Panel A uses all 300 country pairs. Panel B selects country pairs such that their betas are significantly different at least at the 5% confidence level. For more details, see the notes under figure 7.

tions and it includes weekends. Figure B.7 shows that our results are mainly driven by days in which the news are predominantly about transition risk.



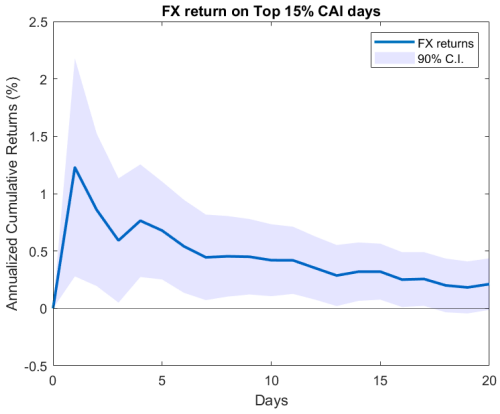
B.5(a) Combine EU



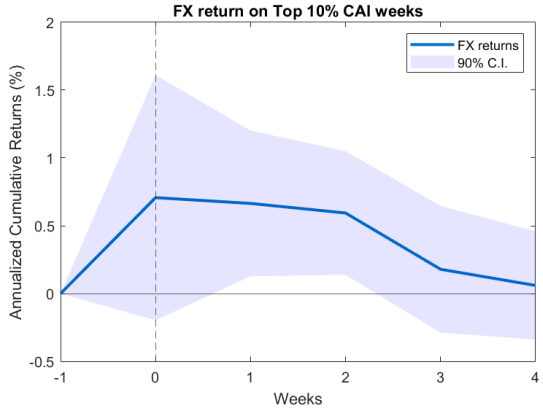
B.5(b) Residual Betas

FIG. B.5. FX AND WORLD CAI: ADDITIONAL ROBUSTNESS.

Notes: Panel (a) shows the average cumulative return in FX rates after days with a positive spike in the global CAI, combining the five EU countries (DE, FR, IT, PT, ES) by averaging their β exposures. Panel (b) uses the residual component of country exposures after regressing on the vulnerability index from the University of Notre Dame to repeat the analysis. See notes to figure 7 for details.



B.6(a) Monthly Data



B.6(b) Weekly Data

FIG. B.6. FX AND INNOVATIONS TO WORLD CAI: FREQUENCY ANALYSIS.

Notes: Panel (a) shows the average cumulative return in exchange rates after days with a positive spike in the global CAI, using monthly data to estimate country exposures instead of quarterly data. Panel (b) shows the average cumulative return after weeks with a positive spike in the global CAI, considering all 300 country pairs and selecting the top-10% weeks. To avoid confounding effects, weeks are chosen so that they do not overlap over a 5-week window. See notes to figure 7 for details.

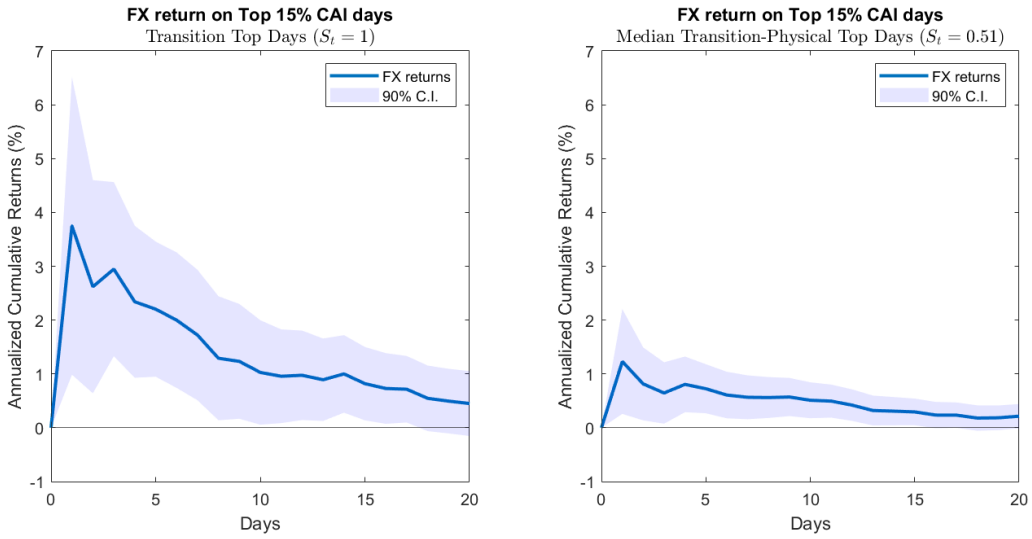


FIG. B.7. FX AND WORLD CAI: TRANSITION VS. PHYSICAL DAYS.

Notes: This figures show the average cumulative return in exchange rates after days with a positive spike in the global CAI. The left (right) panel shows the FX responses conditional on the days that the tweets mostly talk about transition risk (equally talk about both physical and transition risk). The specification is

$$\Delta e^{i,j}_{t,t+k} = a^{i,j}_k + (b_k + c_k \cdot S_t) \cdot \mathbb{1}^{Top}_t + \epsilon^{i,j}_{t,k},$$

where S_t denotes the share of tweets talking about transition risks at day t, normalized between 0 and 1. The responses are constructed using the composite coefficient, $b_k + c_k \cdot S_t$, and by choosing different values of S_t.

Robustness of the equity analysis. Figure B.9 illustrates the distribution of emission intensity across firms, segmented by country. Emission intensity is calculated as the ratio of tons of CO2 emissions to sales, derived from the Trucost dataset. The dataset includes 16,774 firms, providing a comprehensive overview of country-level emission profiles.

Figure B.10 examines the relationship between equity returns and the global Climate Action Index (CAI) using different weighting methods. Panel (a) uses GDP-weighted global CAI to estimate country exposures, while Panel (b) employs Twitter Volume-weighted global CAI. These results are consistent with the analysis presented in the main text (Figure 9), highlighting the robustness of the findings to weighting schemes.

Figure B.11 compares equity returns following days with large positive spikes in the global

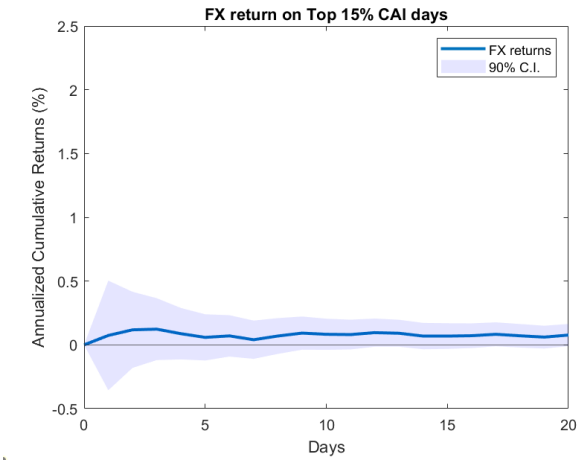


FIG. B.8. FX AND INNOVATIONS TO LOCAL CAI.

Notes: This figure shows the average cumulative return in exchange rates after days with a positive spike in the local CAI, defined as the residual from regressing a country's CAI on the global CAI. Specifically, we estimate

$$\Delta e^{i,j}_{t,t+k} = a^{i,j}_k + b_k \cdot \left(\mathbb{1}^{Top}_{i,t} - \mathbb{1}^{Top}_{j,t} \right) + \epsilon^{i,j}_{t,k},$$

For each country i, the local top-day dummy $\mathbb{1}^{Top}_{i,t}$ is based on the top-15% days of the country's local CAI. See notes to figure 7 for more details.

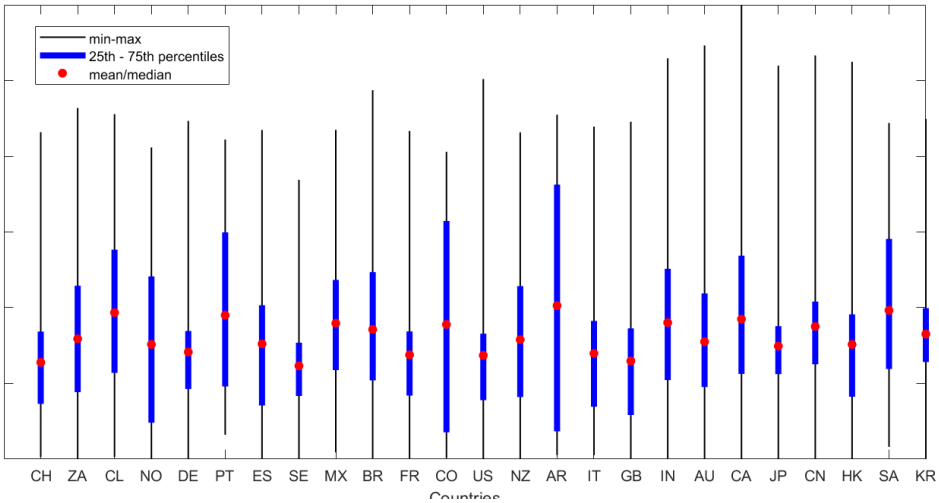
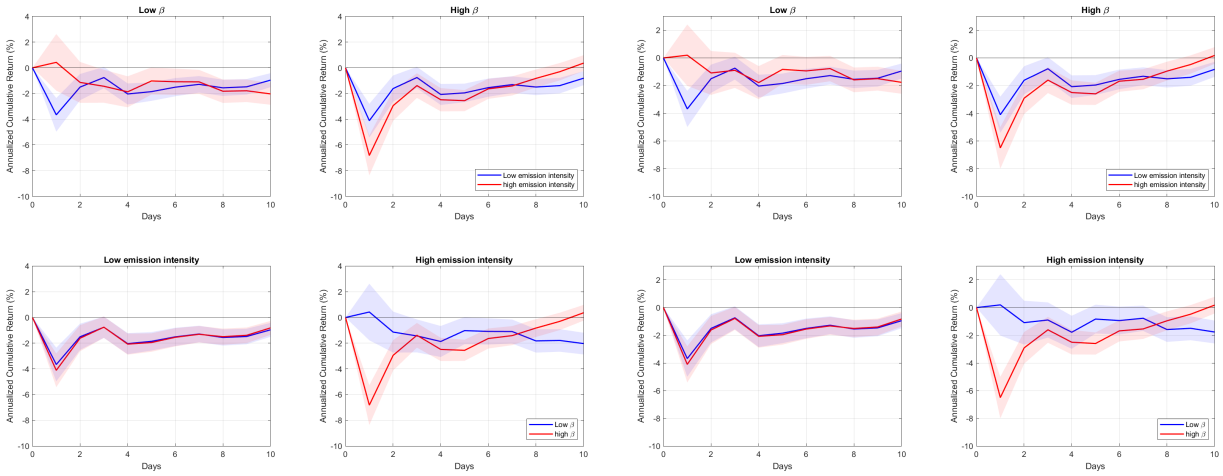


FIG. B.9. EMISSION INTENSITY BY COUNTRY

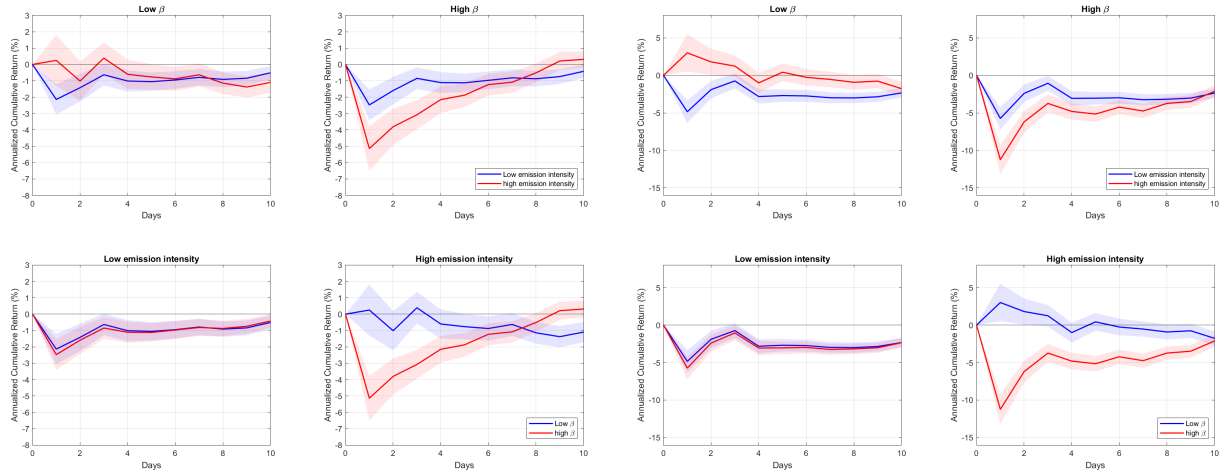
Notes: This figure shows distribution of emission intensity across firms by country. Emission intensity is computed as tons of CO2 divided by sales and it is obtained from the Trucost dataset. We have a total of 16,774 firms.



B.10(a) GDP-Weighted B.10(b) Volume-Weighted

FIG. B.10. EQUITY RETURNS AND WORLD CAI: THE ROLE OF WEIGHTING.

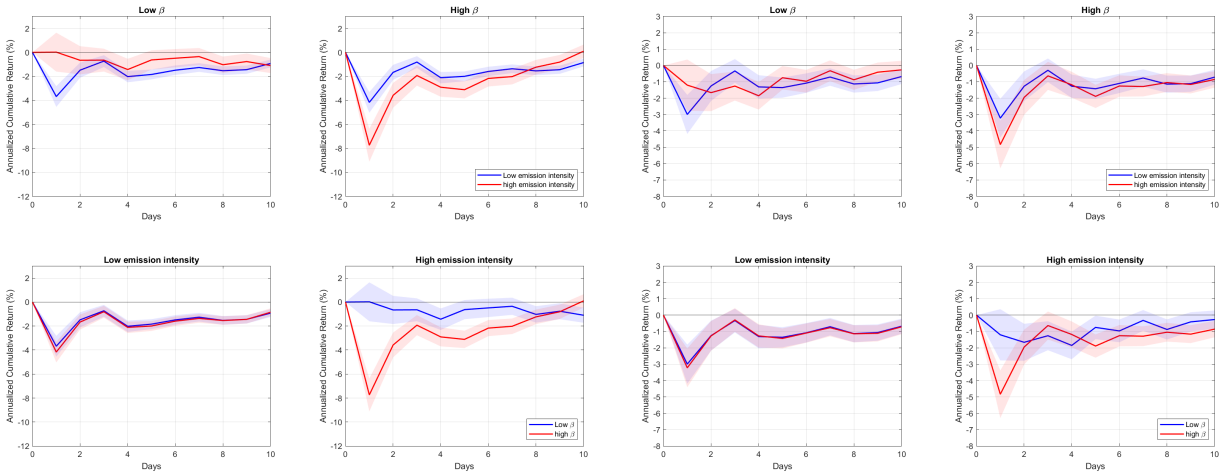
Notes: Panel (a) shows the average cumulative return in equity returns after days with a top-15% positive spike in the global CAI, using the GDP-weighted global CAI to estimate country exposures. Panel (b) shows the results when using the Twitter Volume-weighted global CAI for the same estimation. For more details, see the notes under figure 9.



B.11(a) Top 10% Days B.11(b) Top 20% Days

FIG. B.11. EQUITY RETURNS AND WORLD CAI: TOP 10% VS. TOP 20% DAYS.

Notes: Panel (a) shows the average cumulative return in equity returns after days with a top-10% positive spike in the global CAI. Panel (b) shows the results for days with a top-20% positive spike in the global CAI. For more details, see the notes under figure 9.



B.12(a) Clustered Standard Errors

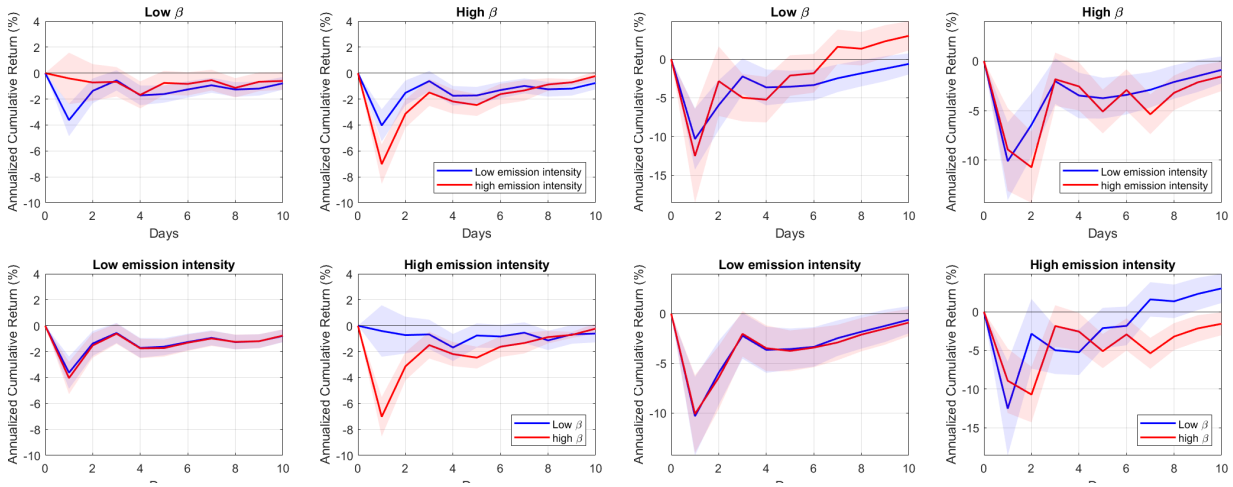
B.12(b) Residual Betas

FIG. B.12. EQUITY RETURNS AND WORLD CAI: ADDITIONAL RESULTS.

Notes: Panel (a) shows the average cumulative return in equity returns after days with a top-15% positive spike in the global CAI, clustering standard errors at the country×industry×date and firm level. Panel (b) shows the results when using residual betas obtained by regressing the exposure coefficients on the vulnerability index from the University of Notre Dame. For more details, see the notes under figure 9.

CAI. Panel (a) focuses on the top-10% of positive spikes, and Panel (b) examines the top-20% of positive spikes. The results align with those reported in the main text (Figure 9), confirming the robustness of the findings of our analysis.

Figure B.12 presents supplementary analyses on equity returns and the global CAI. Panel (a) incorporates clustered standard errors at the country×industry×date and firm level, while Panel (b) uses residual betas derived from regressions of exposure coefficients on the University of Notre Dame's vulnerability index. These findings are consistent with the main text (Figure 9) and provide further validation of the results under alternative methodological specifications.



B.13(a) Median Transition/Physical Top Days

B.13(b) Transition Top Days

FIG. B.13. EQUITY AND WORLD CAI: TRANSITION VS. PHYSICAL DAYS.

Notes: This figure shows the average cumulative return in equity returns after days with a top-15% positive spike in the global CAI, Panel (a) and (b) show the equity return responses conditional on the share of daily tweets related to transition risk being equal to 50% and 100%, respectively. We estimate the following specification

$$\begin{aligned} r^{i,c}_{t,t+k} &= \alpha^i_k + \beta^{i,c}_{t,k} \cdot 1^{Top}_t + \epsilon^{i,c}_{t,k}, \\ \beta^{i,c}_{t,k} &= (\gamma_{0,k} + (\gamma_{1,k} + \gamma_{2,k} \cdot \beta_c) \cdot E_{i,t_a}) + (\kappa_{0,k} + (\kappa_{1,k} + \kappa_{2,k} \cdot \beta_c) \cdot E_{i,t_a}) \cdot S_t, \end{aligned}$$

where S_t denotes the share of tweets talking about transition risks at day t, normalized between 0 and 1. The responses are constructed using the composite coefficient, $\beta^{i,c}_{t,k}$, and by setting $S_t = 0.50$ and $S_t = 1$. For more details, see the notes under figure 9.

Appendix C. Model

In this section, we present both the full description and key derivations of our model. For a more detailed analysis of international models of risk-sharing with recursive preferences and news shows, see Colacito et al. (2018).

C.1 Setup

We generalize the two-period setting presented in Colacito et al. (2018) to include: (i) green investment, and (ii) disutility from pollution. We assume that the intertemporal elasticity of substitution (henceforth IES) is equal to 1 and the preferences are defined as

$$u_t = \begin{cases} (1-\beta)\log\left(C_t D_t^{-a}\right) + \frac{\beta}{1-\gamma}\log E_t\left[\exp\left\{u_{t+1}(1-\gamma)\right\}\right] & \gamma \neq 1 \\ (1-\beta)\log\left(C_t D_t^{-a}\right) + \beta E_t\left[u_{t+1}\right] & \gamma = 1 \end{cases}.$$

A news shock, θ, occurs at $t=1$ about the date $t=2$ productivity of capital. At time $t=1$, uncertainty is resolved and utilities of the home and foreign country are

$$\begin{aligned} u_1 &= (1-\beta)\log\left(C_1 D_1^{-a}\right) + \beta(1-\beta)\log\left(C_2 D_2^{-a}\right) \\ u_1^* &= (1-\beta)\log\left(C_1^* D_1^{*-a}\right) + \beta(1-\beta)\log\left(C_2^* D_2^{*-a}\right) \end{aligned}$$

where

$$C_t = X_t^{\lambda} Y_t^{(1-\lambda)}, \quad C_t^* = X_t^{*(1-\lambda)} Y_t^{*\lambda}$$

$\forall t = \{1,2\}$ denote the consumption bundles, the parameter $a \in (0,1)$ captures the disutility from climate-related damage, and D_t is the amount of damage. The damage depends on both the aggregate output and green investment. Specifically, D_1 and D_1^* are given at $t=1$ and do not depend on the economic activity chosen for time-2. D_2 and D_2^* are the composites of climate-related damage of the home and the foreign country, respectively. They are defined as

$$D_2 = e^{bg}\left(e^z e^{\theta} G/I_g\right)^{\lambda_g}\left(e^{-z} e^{-\theta} G^*/I_g^*\right)^{1-\lambda_g}, \quad D_2^* = e^{g}\left(e^{-z} e^{-\theta} G^*/I_g^*\right)^{\lambda_g}\left(e^z e^{\theta} G/I_g\right)^{1-\lambda_g},$$

where $g \sim N(0,\sigma_g^2)$ is a global climate shock, and b captures the exposure of the home country to it (the exposure of foreign country is normalized to unity). $z \sim N(0,\sigma_z^2)$ is the local climate shock in the home country and it increases the disutility through domestic pollution. $\theta \sim N(0,\sigma_\theta^2)$ is the time-2 productivity shock in the home country, and λ_g captures the home bias

in climate-related damage. G and G^* are aggregation of time $t = 1$ investment for the home and foreign countries and are defined as

$$G = I_{x,1}^{\lambda_I} I_{x,1}^{*1-\lambda_I}, \quad G^* = I_{y,1}^{1-\lambda_I} I_{y,1}^{*\lambda_I}.$$

Time $t = 2$ output in the two countries is determined as $e^{\theta} G$ and $e^{-\theta} G^*$. The budget constraint are

$$1 = X_1 + X_1^* + I_{x,1} + I_{y,1} + I_g, \qquad 1 = Y_1 + Y_1^* + I_{y,1}^* + I_{x,1}^* + I_g^*$$
$$e^{\theta} G = X_2 + X_2^*, \qquad e^{-\theta} G^* = Y_2 + Y_2^*.$$

All shocks are $i.i.d.$

The social planner chooses $\{X_t, X_t^*, Y_t, Y_t^*\}_{t=1,2}$, $I_{x,1}$, $I_{y,1}$, I_g, $I_{y,1}^*$, $I_{x,1}^*$, I_g^* to maximize

$$W = \mu_0 E_0[u_1] + (1 - \mu_0) E_0[u_1^*].$$

Define $S_0 := \frac{\mu_0}{1-\mu_0}$ and let S_1 be the pseudo-Pareto after the news shocks are realized. One can prove that:

$$S_1 = S_0 e^{(u_1 - u_1^*)(1-\gamma)}.$$

C.2 Solution of the Model

Time 2. The optimization problem at $t = 2$ is

$$\max_{X_2, X_2^*, Y_2, Y_2^*} \quad S_2 u_2 + u_2^*$$
$$s.t. \quad e^{\theta} G = X_2 + X_2^*,$$
$$e^{-\theta} G^* = Y_2 + Y_2^*.$$

Note that the objective function can be written as

$$S_2 \left(\lambda \log X_2 + (1-\lambda)\log Y_2 - a \log D_2\right) + \left((1-\lambda)\log X_2^* + \lambda \log Y_2^* - a \log D_2^*\right).$$

The optimal condition will be

$$\frac{S_2 \lambda}{X_2} = \frac{1-\lambda}{X_2^*}, \quad \frac{S_2(1-\lambda)}{Y_2} = \frac{\lambda}{Y_2^*}.$$

Using the condition that $S_2 = S_1$, the solution for home country is

$$X_2 = \frac{\lambda S_1}{1-\lambda+\lambda S_1} e^{\theta} G, \quad Y_2 = \frac{(1-\lambda)S_1}{\lambda + (1-\lambda)S_1} e^{-\theta} G^*.$$

The solution for foreign country follows by symmetry. We can log-linearize this solution around $\bar{s} = 0$ to obtain

$$\log X_2 \approx \log \lambda + (1-\lambda)s_1 + \theta + \log G, \quad \log Y_2 \approx \log(1-\lambda) + \lambda s_1 - \theta + \log G^*.$$

It follows that

$$\begin{aligned}
\log C_2 D_2^{-a} &= const + (2\lambda - 1)\theta + 2\lambda(1-\lambda)s_1 + \lambda \log G + (1-\lambda)\log G^* - a \log D_2 \\
\log C_2^* D_2^{*-a} &= const - (2\lambda - 1)\theta - 2\lambda(1-\lambda)s_1 + (1-\lambda)\log G + \lambda \log G^* - a \log D_2^*
\end{aligned}$$

where

$$\begin{aligned}
\log D_2 &= \lambda_g(\log G - \log I_g + \theta + z) + (1-\lambda_g)(\log G^* - \log I_g^* - \theta - z) + bg \\
\log D_2^* &= \lambda_g(\log G^* - \log I_g^* - \theta - z) + (1-\lambda_g)(\log G - \log I_g + \theta + z) + g.
\end{aligned}$$

Time 1. At date $t=1$, the social planner chooses X_1, X_1^*, Y_1, Y_1^*, $I_{x,1}$, $I_{y,1}$, I_g, $I_{y,1}^*$, $I_{x,1}^*$, I_g^* to

$$\max S_1 \left(\log C_1 + \beta \log C_2 D_2^{-a}\right) + \left(\log C_1^* + \beta \log C_2^* D_2^{*-a}\right)$$

subject to

$$1 = X_1 + X_1^* + I_{x,1} + I_{y,1} + I_g, \quad 1 = Y_1 + Y_1^* + I_{y,1}^* + I_{x,1}^* + I_g^*$$

where we have omitted constant terms (D_1, D_1^*, and $1-\beta$). Define $\hat{\lambda} \equiv \lambda - a\lambda_g$ and expand the expression for the objective function as follows:

$$\begin{aligned} S_1 \Bigg\{ & \lambda \log X_1 + (1-\lambda)\log Y_1 + \beta \Big[(2\lambda-1)\theta + 2\lambda(1-\lambda)s_1 + \hat{\lambda}\left(\lambda_I \log I_{x,1} + (1-\lambda_I) I_{x,1}^*\right) + (1-a-\hat{\lambda}) \\ & \left(\lambda_I \log I_{y,1}^* + (1-\lambda_I)\log I_{y,1}\right) - a\left[-\lambda_g \log I_g - (1-\lambda_g)\log I_g^* + (2\lambda_g - 1)(\theta + z) + bg\right] \Big] \Bigg\} \\ & + \lambda \log Y_1^* + (1-\lambda)\log X_1^* + \beta \Big[-(2\lambda-1)\theta - 2\lambda(1-\lambda)s_1 + (1-a-\hat{\lambda})\left(\lambda_I \log I_{x,1} + (1-\lambda_I) I_{x,1}^*\right) \\ & + \hat{\lambda}\left(\lambda_I \log I_{y,1}^* + (1-\lambda_I)\log I_{y,1}\right) - a\left[-\lambda_g \log I_g^* - (1-\lambda_g)\log I_g - (2\lambda_g - 1)(\theta + z) + g\right] \Big]. \end{aligned}$$

Since the objective function is log-linear and the constraint is linear, the solution for the home country variables is

$$\begin{aligned} X_1 &= \frac{1}{K} S_1 \lambda, \qquad X_1^* = \frac{1}{K}(1-\lambda) \\ I_{x,1} &= \frac{\beta \lambda_I}{K}\left(S_1 \hat{\lambda} + 1 - a - \hat{\lambda}\right), \qquad I_{y,1} = \frac{\beta(1-\lambda_I)}{K}\left(S_1(1-a-\hat{\lambda}) + \hat{\lambda}\right) \\ I_g &= \frac{\beta a}{K}\left(S_1 \lambda_g + 1 - \lambda_g\right), \end{aligned}$$

where

$$K = 1 - \lambda + \beta\lambda_I(1-a-\hat{\lambda}) + \beta(1-\lambda_I)\hat{\lambda} + \beta a(1-\lambda_g) + \left[\lambda + \beta\lambda_I\hat{\lambda} + \beta(1-\lambda_I)(1-a-\hat{\lambda}) + \beta a \lambda_g\right] S_1$$

After log-linearizing these expressions, we get

$$\begin{aligned}
\log X_1 &\approx \log\frac{\lambda}{1+\beta} + \underbrace{\frac{1-\lambda+\beta\lambda_I(1-a-\hat{\lambda})+\beta(1-\lambda_I)\hat{\lambda}+\beta a(1-\lambda_g)}{1+\beta}}_{\lambda_x^s} s_1 \\
\log X_1^* &\approx \log\frac{1-\lambda}{1+\beta} + \underbrace{(\lambda_x^s-1)}_{\lambda_{x^*}^s} s_1 \\
\log I_{x,1} &\approx \log\frac{\beta\lambda_I(1-a)}{1+\beta} + \underbrace{\left(\frac{a(\lambda-\lambda_g)}{1-a}+\frac{\beta(1-\lambda_I)\left(2\hat{\lambda}-(1-a)\right)}{1+\beta}\right)}_{\lambda_{I_x}^s} s_1 \\
\log I_{y,1} &\approx \log\frac{\beta(1-\lambda_I)(1-a)}{1+\beta} + \underbrace{\left(\frac{a(\lambda-\lambda_g)}{1-a}+\frac{(1+\beta a+\beta\lambda_I(1-a))\left(1-a-2\hat{\lambda}\right)}{(1+\beta)(1-a)}\right)}_{\lambda_{I_y}^s} s_1 \\
\log I_g &\approx \log\frac{\beta a}{1+\beta} + \underbrace{\left(\lambda_g-\lambda+\frac{\beta(1-\lambda_I)\left(2\hat{\lambda}-(1-a)\right)}{1+\beta}\right)}_{\lambda_{I_g}^s} s_1.
\end{aligned}$$

By symmetry,

$$\log Y_1 \approx \log\frac{1-\lambda}{1+\beta} - \lambda_{x^*}^s s_1, \quad \log Y_1^* \approx \log\frac{\lambda}{1+\beta} - \lambda_x^s s_1$$

$$\log I_{x,1}^* \approx \log\frac{\beta(1-\lambda_I)(1-a)}{1+\beta} - \lambda_{I_y}^s s_1, \quad \log I_{y,1}^* \approx \log\frac{\beta\lambda_I(1-a)}{1+\beta} - \lambda_{I_x}^s s_1$$

$$\log I_g^* \approx \log\frac{\beta a}{1+\beta} - \lambda_{I_g}^s s_1.$$

Sensitivity of pareto weights to the shocks. The utility function is characterized as

$$u_1 = const + \lambda_u^\theta\theta + \lambda_u^z z + b\lambda_u^g g + \lambda_u^s s_1 = const + \underbrace{\left(\lambda_u^\theta + \lambda_u^s\lambda_s^\theta\right)}_{\lambda_\theta}\theta + \underbrace{(\lambda_u^z + \lambda_u^s\lambda_s^z)}_{\lambda_z} z + \underbrace{(b\lambda_u^g + \lambda_u^s\lambda_s^g)}_{\lambda_g} g$$

$$u_1^* = const - \lambda_u^\theta\theta - \lambda_u^z z + \lambda_u^g g - \lambda_u^s s_1 = const - \left(\lambda_u^\theta + \lambda_u^s\lambda_s^\theta\right)\theta - \left(\lambda_u^z + \lambda_u^s\lambda_s^z\right) z - \left(-\lambda_u^g + \lambda_u^s\lambda_s^g\right) g$$

where

$$
\begin{aligned}
\lambda_u^\theta &= \beta(1-\beta)\left(2\lambda - 1 - a(2\lambda_g - 1)\right) = \beta(1-\beta)\left(2\hat{\lambda} - (1-a)\right) \\
\lambda_u^z &= -\beta(1-\beta)a\left(2\lambda_g - 1\right) \\
\lambda_u^g &= -\beta(1-\beta)a \\
\lambda_u^s &= (1-\beta)\left(\lambda\lambda_x^s - (1-\lambda)\lambda_{x^*}^s\right) \\
&\quad +(1-\beta)\beta\left(2\lambda(1-\lambda) + (2\hat{\lambda} - 1 + a)\left(\lambda_I\lambda_{I_x}^s - (1-\lambda_I)\lambda_{I_y}^s\right) + a(2\lambda_g - 1)\lambda_{I_g}^s\right)
\end{aligned}
$$

Notice that $s_1 = (u_1 - u_1^*)(1-\gamma)$. Thus $\lambda_s^\theta = 2(1-\gamma)\lambda_\theta$, $\lambda_s^z = 2(1-\gamma)\lambda_z$, and $\lambda_s^g = (1-\gamma)\left((b-1)\lambda_u^g + 2\lambda_u^s\lambda_s^g\right)$. As a result, we get:

$$
\lambda_s^\theta = \frac{2(1-\gamma)\lambda_u^\theta}{1 + 2(\gamma-1)\lambda_u^s}, \quad \lambda_s^z = \frac{2(1-\gamma)\lambda_u^z}{1 + 2(\gamma-1)\lambda_u^s}, \quad \lambda_s^g = \frac{(1-\gamma)(b-1)\lambda_u^g}{1 + 2(\gamma-1)\lambda_u^s}.
$$

Next we examine how the ratio of the pseudo Pareto weights responds to different shocks.

Assumption 1. *Assume home bias in both consumption and cliamte-related damage, that is,* $0.5 < \lambda, \lambda_g < 1$. *In addition, assume* $\frac{1-a}{2} < \hat{\lambda} < 1 - a$ *(home bias in the consumption-damage composite).*

Lemma 1. *Given assumption 1, then*

1. $\lambda_x^s > 0$, $\lambda_{x^*}^s < 0$, $\lambda_{I_y}^s < 0$
2. $\lambda_{I_x}^s > 0$ *when* $\lambda > \lambda_g$, *otherwise it can be either positive or negative*
3. $\lambda_{I_g}^s > 0$ *when* $\lambda < \lambda_g$, *otherwise it can be either positive or negative*

In summary, the sign of these variables are given below

	$\lambda > \lambda_g$	$\lambda < \lambda_g$
λ_x^s	+	+
$\lambda_{x^*}^s$	-	-
$\lambda_{I_x}^s$	+	Undetermined
$\lambda_{I_y}^s$	-	-
$\lambda_{I_g}^s$	Undetermined	+

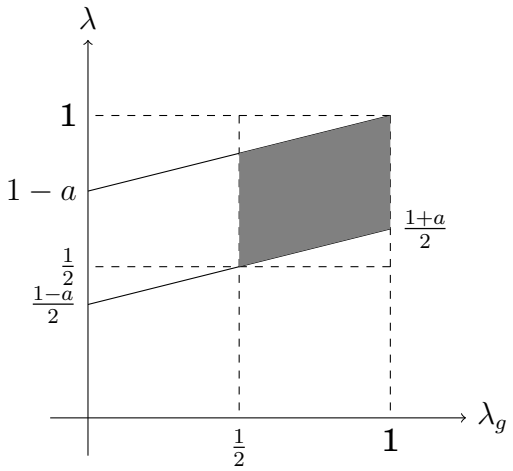


FIG. C.14. ASSUMPTION ON λ_g AND λ

Proof.

1. Given that $\lambda, \lambda_g < 1$ and $\hat{\lambda} < 1 - a$, we can easily verify that $\lambda_x^s > 0$

2. Given that

$$1-\lambda+\beta\lambda_I(1-a-\hat{\lambda})+\beta(1-\lambda_I)\hat{\lambda}+\beta a(1-\lambda_g) < 1+\beta\lambda_I(1-a)+\beta(1-\lambda_I)(1-a)+\beta a = 1+\beta$$

   We know $\lambda_x^s < 1$, thus $\lambda_{x^*}^s = \lambda_x^s - 1 < 0$

3. $\lambda_{I_x}^s = \frac{a(\lambda-\lambda_g)}{1-a} + \frac{\beta(1-\lambda_I)\left(2\hat{\lambda}-(1-a)\right)}{1+\beta}$. If $\lambda > \lambda_g$ and given $\hat{\lambda} > \frac{1-a}{2}$, we have $\lambda_{I_x}^s > 0$. Otherwise we can have negative values.

4. Note that

$$\begin{aligned}
\lambda_{I_y}^s &= \frac{(1+\beta)a(\lambda-\lambda_g)+(1+\beta a)(1-a-2\hat{\lambda})+\beta\lambda_I(1-a)(1-a-2\hat{\lambda})}{(1+\beta)(1-a)} \\
&= \frac{a(\lambda-\lambda_g)+1-a-2\hat{\lambda}+\beta\lambda_I(1-a)(1-a-2\hat{\lambda})+\beta a(1-a-2\hat{\lambda}+\lambda-\lambda_g)}{(1+\beta)(1-a)} \\
&= \frac{(1-\lambda)(1-a)-\hat{\lambda}+\beta\lambda_I(1-a)(1-a-2\hat{\lambda})+\beta a\left((1-\lambda_g)(1-a)-\hat{\lambda}\right)}{(1+\beta)(1-a)}.
\end{aligned}$$

Since $(1-\lambda)(1-a) < \frac{1-a}{2}$, $(1-\lambda_g)(1-a) < \frac{1-a}{2}$, and $\hat{\lambda} > \frac{1-a}{2}$, the numerator is negative. Thus $\lambda^s_{I_y} < 0$.

5. $\lambda^s_{I_g} = \lambda_g - \lambda + \frac{\beta(1-\lambda_I)\left(2\hat{\lambda}-(1-a)\right)}{1+\beta}$. When $\lambda < \lambda_g$, since $\hat{\lambda} > \frac{1-a}{2}$, we have $\lambda^s_{I_g} > 0$. Otherwise we can have negative values.

□

Lemma 2. *Since $\lambda^s_u > 0$, when $\gamma > 1$ we have: (i) $\lambda^\theta_s < 0$ and $\lambda^z_s > 0$, and (ii) $\lambda^g_s > 0$ (< 0) if $b > 1$ (< 1).*

Proof.

1. When $\lambda > \lambda_g$, we need to prove that the negative part related to $\lambda^s_{I_g}$ does not prevail on the positive part. From $(1-\beta)\left(\lambda\lambda^s_x - (1-\lambda)\lambda^s_{x^*}\right)$ we can extract $(1-\beta)(1-\lambda) > 0$ (since $\lambda^s_{x^*} = \lambda^s_x - 1$) and the leave the remaining part positive. The negative part from $\lambda^s_{I_g}$ is $(1-\beta)\beta a(2\lambda_g - 1)(\lambda_g - \lambda)$. Thus we need to prove

$$1 - \lambda + \beta a(2\lambda_g - 1)(\lambda_g - \lambda) > 0$$

when all parameter satisfies the assumption 1. Note that $\hat{\lambda} < 1 - a$ also means:

$$\lambda < 1 - a + a\lambda_g.$$

Then

$$\begin{aligned} 1 - \lambda + \beta a(2\lambda_g - 1)(\lambda_g - \lambda) &> 1 - (1 - a + a\lambda_g) + \beta a(2\lambda_g - 1)\left(\lambda_g - (1 - a + a\lambda_g)\right) \\ &= a(1-\lambda_g) + \beta a(2\lambda_g - 1)(1-a)(\lambda_g - 1) \\ &= a(1-\lambda_g)\left(1 - \beta(2\lambda_g - 1)(1-a)\right) \\ &> 0, \end{aligned}$$

where the last inequality holds since $\beta < 1$, $2\lambda_g - 1 < 1$, and $1 - a < 1$.

2. When $\lambda < \lambda_g$, we need to prove that the negative part related to $\lambda^s_{I_x}$ does not prevail on the positive part. The negative part is $(1-\beta)\beta(2\hat{\lambda} - 1 + a)\lambda_I \frac{a}{1-a}(\lambda - \lambda_g)$. As before, the positive part $(1-\beta)(1-\lambda) > 0$ so that we need to prove

$$1 - \lambda > \beta(2\hat{\lambda} - 1 + a)\lambda_I \frac{a}{1-a}(\lambda_g - \lambda).$$

Note that $\frac{2\hat{\lambda}-1+a}{1-a} = \frac{2\hat{\lambda}}{1-a} - 1 < 1$ since $\hat{\lambda} < 1 - a$. Then $\beta(2\hat{\lambda} - 1 + a)\lambda_I \frac{a}{1-a}(\lambda_g - \lambda) < \beta a \lambda_I(\lambda_g - \lambda) < \lambda_g - \lambda < 1 - \lambda$.

Since $\lambda^u_s > 0$, and

$$\lambda^\theta_u = \beta(1-\beta)\left(2\hat{\lambda} - (1-a)\right) > 0$$

$$\lambda^z_u = -\beta(1-\beta)a\left(2\lambda_g - 1\right) < 0$$

$$\lambda^g_u = -\beta(1-\beta)a < 0$$

it is immediate that $\lambda^\theta_s < 0$ and $\lambda^z_s > 0$ when $\gamma > 1$. In addition, when $b > 1$ (< 1), $\lambda^g_s > 0$ (< 0). □

C.3 Implications

Net export and green investment. According to the definition of net export of consumption and investment

$$\frac{NX^C_1}{X_1} = \frac{X^*_1}{X_1} - \left(\frac{1-\lambda}{\lambda}\frac{X_1}{Y_1}\right)\frac{Y_1}{X_1} = \frac{1-\lambda}{\lambda}\left(\frac{1}{S_1} - 1\right)$$

$$\frac{NX^I_1}{I_x} = \frac{I_y}{I_x} - \left(\frac{1-\lambda_i}{\lambda_i}\frac{I_x}{I^*_x}\right)\frac{I^*_x}{I_x} = \frac{1-\lambda_i}{\lambda_i}\left(\frac{S_1 + \hat{\kappa}}{\hat{\kappa}S_1 + 1} - 1\right)$$

where $\hat{\kappa} = \frac{\hat{\lambda}}{1-a-\hat{\lambda}} = \frac{\lambda - a\lambda_g}{1-\lambda-a(1-\lambda_g)} > 1$. Thus

Proposition 4. *A positive productivity news shock θ decreases the pseudo Pareto weight of home country S_1, and it*

1. *increases the net export of consumption and investment goods, $\frac{NX_1^C}{X_1}$ and $\frac{NX_1^I}{I_x}$*
2. *decreases green investment I_g when $\lambda_g > \lambda$*

Proposition 5. *A positive **local** climate shock z increases the pseudo Pareto weight of home country S_1, and it*

1. *decreases the net export of consumption and investment goods, $\frac{NX_1^C}{X_1}$ and $\frac{NX_1^I}{I_x}$*
2. *increases green investment I_g when $\lambda_g > \lambda$*

Proposition 6. *When $b > 1$, a positive **global** climate shock g increases the pseudo Pareto weight of home country S_1, and it*

1. *decreases the net export of consumption and investment goods, $\frac{NX_1^C}{X_1}$ and $\frac{NX_1^I}{I_x}$*
2. *increases green investment I_g when $\lambda_g > \lambda$*

Exchange rate. Note that the Pareto weight satisfies

$$S_1 = S_0 \frac{M_1}{M_1^*} \frac{e^{\Delta c_1}}{e^{\Delta c_1^*}}$$

where M_1 and M_1^* are the SDFs of home and foreign country, respectively. Taking the logarithm,

$$s_1 = s_0 + m_1 - m_1^* + \Delta c_1 - \Delta c_1^*$$

Note that $\Delta e_1 = m_1 - m_1^*$, where Δe_1 is the log change of real exchange rate (amount of foreign currency per unit of domestic currency). Given that s_0, c_0, and c_0^* are constant that do

not depend on the shocks,

$$\begin{aligned}
\Delta e_1 &= const + s_1 - c_1 + c_1^* \\
&= const + s_1 - (\lambda \log X_1 + (1-\lambda)\log Y_1) + (\lambda \log Y_1^* + (1-\lambda)\log X_1^*) \\
&= const + s_1 - (\lambda\lambda_x^s - (1-\lambda)\lambda_{x^*}^s)\, s_1 + (-\lambda\lambda_x^s + (1-\lambda)\lambda_{x^*}^s)\, s_1 \\
&= const + \underbrace{(1 - 2\,(\lambda\lambda_x^s - (1-\lambda)\lambda_{x^*}^s))}_{\lambda_e^s}\, s_1
\end{aligned}$$

Thus there is a one-to-one mapping between the pseudo-Pareto weight s_1 and the changes in the real exchange rate. The relation depends on the sign of λ_e^s. The following lemma shows that $\lambda_e^s > 0$ under Assumption 1.

Lemma 3. *Given Assumption 1,* $\lambda_e^s > 0$.

Proof. Note that $\lambda_{x^*}^s = \lambda_x^s - 1$, we need to show that

$$\lambda_e^s = 1 - 2(\lambda\lambda_x^s - (1-\lambda)(\lambda_x^s - 1)) = 1 - 2((2\lambda - 1)\lambda_x^s - (1-\lambda)) > 0$$

which indicates $(2\lambda - 1)\lambda_x^s < \frac{3}{2} - \lambda$. Substituting it with the expression of λ_x^s,

$$(2\lambda - 1)\left(1 - \lambda + \beta\lambda_I(1 - a - \hat{\lambda}) + \beta(1-\lambda_I)\hat{\lambda} + \beta a(1-\lambda_g)\right) < \left(\frac{3}{2} - \lambda\right)(1+\beta)$$

Note that

$$\begin{aligned}
& \beta\lambda_I(1 - a - \hat{\lambda}) + \beta(1-\lambda_I)\hat{\lambda} + \beta a(1-\lambda_g) \\
< \;& \beta\lambda_I(1-a) + \beta(1-\lambda_I)(1-a) + \beta a \\
= \;& \beta(1-a) + \beta a \\
= \;& \beta.
\end{aligned}$$

Thus the inequality that we need to prove reduces to

$$\begin{aligned}(2\lambda-1)(1-\lambda+\beta) &< \left(\frac{3}{2}-\lambda\right)(1+\beta)\\ (2\lambda-1)(1+\beta)-(2\lambda-1)\lambda &< \left(\frac{3}{2}-\lambda\right)(1+\beta)\\ \left(3\lambda-\frac{5}{2}\right)(1+\beta) &< (2\lambda-1)\lambda.\end{aligned}$$

If $\frac{1}{2}<\lambda<\frac{5}{6}$, the inequality holds immediately. If not, we adopt the implicit assumption that the subjective discount rate β is less than one. Then we only need to prove

$$6\lambda-5<(2\lambda-1)\lambda \quad \Rightarrow \quad (2\lambda-5)(\lambda-1)>0$$

This inequality holds because $\lambda<1$. □

Proposition 7. *There is a positive one-to-one mapping between s_1 and the log growth of the real exchange rate Δe_1. Hence any shock that moves s_1 upward affects Δe_1 in the same direction.*

Stochastic discount factor. Let's examine how the stochastic discount factor responds to different shocks. Note that for the home country, the SDF at time 1 is given by

$$M_1=\frac{\partial u_0/\partial C_1}{\partial u_0/\partial C_0}$$

where u_0 is the utility at time 0,

$$u_0=(1-\beta)\log C_0 D_0^{-\alpha}+\frac{\beta}{1-\gamma}\log E_0\left[\exp\left\{u_1(1-\gamma)\right\}\right]$$

As a result, we get:

$$M_1=\beta\frac{C_0}{C_1}\frac{\exp\left(u_1(1-\gamma)\right)}{E_0\left[\exp\left(u_1(1-\gamma)\right)\right]},$$

and in log-units:

$$m_1 = \log(\beta) + \log(C_0) - \log(C_1) + (1-\gamma)u_1 - \log E_0\left[\exp\left(u_1(1-\gamma)\right)\right].$$

Substituting the expressions of $\log C_1$ and u_1,

$$m_1 = const - (\lambda\lambda_x^s - (1-\lambda)\lambda_{x^*}^s)s_1 + (1-\gamma)(\lambda_\theta\theta + \lambda_z z + \lambda_g g),$$

where all time-0 terms end up in the constant. In addition, note that

$$(1-\gamma)\lambda_\theta = \frac{1}{2}\lambda_s^\theta, \quad (1-\gamma)\lambda_z = \frac{1}{2}\lambda_s^z$$

$$(1-\gamma)\lambda_g = (1-\gamma)\left(b\lambda_u^g + \lambda_u^s\lambda_s^g\right) = \underbrace{(1-\gamma)\left(\frac{b-1}{2}\lambda_u^g + \lambda_u^s\lambda_s^g\right)}_{\frac{1}{2}\lambda_s^g} + (1-\gamma)\frac{b+1}{2}\lambda_u^g.$$

Thus

$$m_1 = const + \underbrace{\left(\frac{1}{2} - (\lambda\lambda_x^s - (1-\lambda)\lambda_{x^*}^s)\right)}_{\frac{1}{2}\lambda_e^s} s_1 + \frac{1}{2}(1-\gamma)(1+b)\lambda_u^g g.$$

Similarly, the SDF for the foreign country is

$$m_1^* = const - \frac{1}{2}\lambda_e^s s_1 + \frac{1}{2}(1-\gamma)(1+b)\lambda_u^g g$$

The expressions of two SDFs also verifies that

$$\Delta e_1 = m_1 - m_1^* = const + \lambda_e^s s_1$$

We have shown that $\lambda_e^s > 0$ in Lemma 3. In addition, $\lambda_u^g = -\beta(1-\beta)a < 0$. Hence if we hold the Pareto weight constant, a global climate shock increases the SDFs for both countries.

Proposition 8. *Holding g constant, there is a one-to-one mapping between the SDF and the*

pseudo-Pareto weight s_1. An increase in s_1 corresponds to an increase in m_1 (a decrease in m_1^*).

Thus both the productivity shock θ and the local climate shock z have an unambiguous effect on the SDF of the two countries. The effect of the global climate shock g is unambiguous conditional on the following parameter restrictions.

Proposition 9. *Let $\gamma > 1$, when $b > 1$ ($b < 1$), a positive global climate news shock increases the SDF of the home (foreign) country.*

C.4 Additional Results with Empirical Predictions

In this section, we develop additional testable predictions that guide our empirical design.

C.4.1 Net exports.

For the home country, net export for consumption goods is

$$\frac{NX_1^C}{X_1} = \frac{1-\lambda}{\lambda}\left(\frac{1}{S_1} - 1\right) = const - \frac{1-\lambda}{\lambda} e^{-\bar{s}_1} s_1$$

By symmetry, net export of the foreign country is

$$\frac{NX_1^{C*}}{Y_1^*} = \frac{1-\lambda}{\lambda}\left(S_1 - 1\right) = const + \frac{1-\lambda}{\lambda} e^{\bar{s}_1} s_1.$$

Thus

$$\frac{NX_1^C}{X_1} - \frac{NX_1^{C*}}{Y_1^*} = const - \frac{1-\lambda}{\lambda}(e^{\bar{s}_1} - e^{-\bar{s}_1}) s_1$$

Given that

$$s_1 = \bar{s}_1 + \lambda_s^\theta \theta + \lambda_s^g g + \lambda_s^z z$$

Then

$$\frac{NX_1^C}{X_1} - \frac{NX_1^{C*}}{Y_1^*} = const + \beta_\theta^{NX} \cdot 2\theta + \beta_g^{NX}(b-1)g + \beta_z^{NX} \cdot 2z$$

where, according to Lemma 2,

$$\begin{aligned}
\beta_\theta^{NX} &= -\frac{1}{2}\frac{1-\lambda}{\lambda}(e^{\bar{s}_1} - e^{-\bar{s}_1})\lambda_s^\theta > 0 \\
\beta_g^{NX} &= -\frac{1}{2}\frac{1-\lambda}{\lambda}(e^{\bar{s}_1} - e^{-\bar{s}_1})\frac{\lambda_s^g}{b-1} < 0 \\
\beta_z^{NX} &= -\frac{1}{2}\frac{1-\lambda}{\lambda}(e^{\bar{s}_1} - e^{-\bar{s}_1})\lambda_s^z < 0
\end{aligned}$$

Similarly, the relation holds for net export of investment goods.

C.4.2 Foreign exchange rate.

The log growth of real foreign exchange rate (number of foreign currencies per unit of home currency) is

$$\Delta e_1 = m_1 - m_1^* = const + \lambda_e^s s_1$$

where $\lambda_e^s > 0$ according to Lemma 3. Then

$$\Delta e_1 = const + \beta_\theta^{FX} \cdot 2\theta + \beta_g^{FX} \cdot (b-1)g + \beta_z^{FX} \cdot 2z$$

where

$$\begin{aligned}
\beta_\theta^{FX} &= \frac{1}{2}\lambda_e^s\lambda_s^\theta < 0 \\
\beta_g^{FX} &= \frac{1}{2}\lambda_e^s\frac{\lambda_s^g}{b-1} > 0 \\
\beta_z^{FX} &= \frac{1}{2}\lambda_e^s\lambda_s^z > 0
\end{aligned}$$

C.4.3 Cross section of returns

We characterize the returns to both brown and green capital in the home country. We choose the home country because its exposure to climate news, b, can take values other than 1. In this two-period model, we focus on investment returns at $t = 1$ and derive their exposure coefficients with respect to our exogenous shocks. In particular, we define the returns as follows

$$R_{i,t=1} = \frac{PV_{i,t=1}}{PV_{i,t=0}} = \frac{E_1\left(SDF_{1,2} \cdot \text{Total dividend of } I_i \text{ at } t=2\right)}{E_0\left(SDF_{0,2} \cdot \text{Total dividend of } I_i \text{ at } t=2\right)} \tag{C.1}$$

where $PV_{i,t}$ denotes the time-t present value of total dividend of investment $i \in \{x, g\}$ generated at the final period of the model. SDF_{t_1,t_2} is the stochastic discount factor from period t_1 to t_2.

Note that the shocks are known at $t = 1$. Thus all uncertainty is fully resolved at $t = 1$ and the stochastic discount factor $SDF_{1,2} = \frac{1}{R_f} = 1$. The last equality follows from our decision to normalize the risk-free rate to be one.

We log-linearize the returns for both green and brown stocks. In practice, we focus on the log-linearization of the numerator in equation (C.1), $PV_{i,t=1}$, as we are mainly interested in the exposure of returns to fundamental shocks. The denominator determines the equilibrium risk premium which is constant in our model.

Brown investment returns. The time-1 present value of total dividends of $I_{x,1}$ is defined as follows:

$$PV_{x,t=1} = Q_x e^{\theta} G \frac{\partial \tilde{C}_2}{\partial X_2},$$

where Q_x is the shadow price per unit of the brown investment, expressed in the unit of home good X. The second term, $e^{\theta}G$, denotes the total output of the home country. The last term, $\frac{\partial \tilde{C}_2}{\partial X_2}$, converts the present value into the unit of composite consumption $\tilde{C}_2 = C_2 D_2^{-a}$, which takes into account the negative effect of pollution.

Since in this model $Q_x = \frac{1}{G_{I_{x,1}}}$, we can write what follows:

$$PV_{x,t=1} = \frac{\lambda}{\lambda_I} \frac{I_{x,1}}{X_2} e^{\theta} \tilde{C}_2.$$

The log-linear brown return is:

$$r_{x,1} = constant + \theta + \log I_{x,1} - \log X_2 + \log \tilde{C}_2. \tag{C.2}$$

Green investment returns. Green investment helps alleviating the damage caused by pollution, thus its dividend is generated from a lower damage D_2 and hence a higher composite consumption bundle, $\tilde{C}_2$. The present value of green investment expressed in units of composite consumption $\tilde{C}$ is:

$$PV_{g,t=1} = I_g \frac{\partial D_2}{\partial I_g} \frac{\partial \tilde{C}_2}{\partial D_2} = a\lambda_g \tilde{C}_2$$

The implied green log-linear return is:

$$r_{g,1} = constant + \log \tilde{C}_2. \tag{C.3}$$

The brown-minus-green return. We examine the heterogeneous exposure of brown and green returns to a global climate shock by constructing the brown-minus-green investment return. Given Equations C.2 and C.3,

$$r_{x,1} - r_{g,1} = constant + \theta + \log I_{x,1} - \log X_2$$

Note that X_2 can be log-linearized as follows

$$\log X_2 \approx \log \lambda + (1-\lambda) s_1 + \theta + \lambda_I \log I_{x,1} + (1-\lambda_I) \log I^*_{x,1}.$$

As a result, we get

$$r_{x,1} - r_{g,1} = constant - (1-\lambda)s_1 + (1-\lambda_I)\left(\log I_{x,1} - \log I^*_{x,1}\right).$$

Since

$$\log I_{x,1} \approx \log \frac{\beta\lambda_I(1-a)}{1+\beta} + \underbrace{\left(\frac{a(\lambda-\lambda_g)}{1-a} + \frac{\beta(1-\lambda_I)\left(2\hat{\lambda}-(1-a)\right)}{1+\beta}\right)}_{\lambda^s_{I_x}} s_1,$$

and

$$\log I^*_{x,1} \approx \log \frac{\beta(1-\lambda_I)(1-a)}{1+\beta} - \lambda^s_{I_y} s_1,$$

we obtain the following result:

$$r_{x,1} - r_{g,1} = constant + \left[\underbrace{(1-\lambda_I)\left(\lambda^s_{I_x} + \lambda^s_{I_y}\right) - (1-\lambda)}_{\lambda^s_{r_x - r_b}}\right] s_1.$$

Hence the green-minus-brown return adjustments are solely driven by the pseudo-Pareto weight s_1.

Lemma 4. *Given Assumption 1,* $(1-\lambda_I)\left(\lambda^s_{I_x} + \lambda^s_{I_y}\right) - (1-\lambda) < 0$*, that is, the brown-minus-green return decreases when the pseudo-Pareto weight increases.*

Proof. Given the formula for $\lambda^s_{I_x}$ and $\lambda^s_{I_y}$, we can get

$$\lambda^s_{I_x} + \lambda^s_{I_y} = \frac{[\beta(1-a)(1-2\lambda_I) - 1 - \beta a]\left(2\hat{\lambda}-(1-a)\right) + 2a(1+\beta)(\lambda-\lambda_g)}{(1+\beta)(1-a)}.$$

As a result, $\lambda^s_{r_x - r_b}$ reduces to:

$$
\begin{aligned}
& (1-\lambda_I)\left(\lambda^s_{I_x} + \lambda^s_{I_y}\right) - (1-\lambda) \\
= & \frac{(1-\lambda_I)\left\{[\beta(1-a)(1-2\lambda_I) - 1 - \beta a]\left(2\hat{\lambda} - (1-a)\right) + 2a(1+\beta)(\lambda - \lambda_g)\right\} - (1-\lambda)(1+\beta)(1-a)}{(1+\beta)(1-a)} \\
= & \frac{(1+\beta)\Big(2a(\lambda-\lambda_g)(1-\lambda_I) - (1-a)(1-\lambda)\Big) + (1-\lambda_I)\left[\beta(1-a)(1-2\lambda_I) - 1 - \beta a\right]\left(2\hat{\lambda} - (1-a)\right)}{(1+\beta)(1-a)}
\end{aligned}
$$

We analyze the sign of this expression step-by-step. The denominator is positive. The second term of the numerator is negative since $1-\lambda_I > 0$, $1 - 2\lambda_I < 0$, and $2\hat{\lambda} - (1-a) > 0$. In order to prove that $\lambda^s_{r_x - r_b} < 0$, we must prove that $2a(\lambda - \lambda_g)(1-\lambda_I) - (1-a)(1-\lambda) < 0$. We do it in what follows:

$$
\begin{aligned}
& 2a(\lambda-\lambda_g)(1-\lambda_I) - (1-a)(1-\lambda) \\
< & \; 2a(\lambda-\lambda_g)(1-\lambda_I) - 2(1-\lambda_I)(1-a)(1-\lambda) \\
= & \; 2(1-\lambda_I)\Big(a(\lambda-\lambda_g) - (1-a)(1-\lambda)\Big) \\
= & \; 2(1-\lambda_I)\left(\hat{\lambda} - (1-a)\right) \\
< & \; 0
\end{aligned}
$$

The first inequality is due to $2(1-\lambda_I) < 1$ and $(1-a)(1-\lambda) > 0$. The second inequality follows from Assumption 1. □

Note that the pseudo-Pareto weight depends on the shocks with the following linear functional form

$$s_1 = \lambda^\theta_s \theta + \lambda^g_s g + \lambda^z_s z$$

where

$$\lambda^\theta_s = \frac{2(1-\gamma)\lambda^\theta_u}{1 + 2(\gamma-1)\lambda^s_u}$$

$$\lambda_s^g = \frac{(1-\gamma)(b-1)\lambda_u^g}{1+2(\gamma-1)\lambda_u^s}$$

$$\lambda_s^z = \frac{2(1-\gamma)\lambda_u^z}{1+2(\gamma-1)\lambda_u^s}$$

Therefore,

$$r_{x,1} - r_{g,1} = constant + \lambda^s_{r_x - r_b}\lambda_s^\theta \theta + \lambda^s_{r_x - r_b}\lambda_s^g g + \lambda^s_{r_x - r_b}\lambda_s^z z \tag{C.4}$$

Given our results in Lemma 2, we obtain the following proposition:

Proposition 10. *If $b > 1$, the brown-minus-green investment return in the home country depreciates when there is a positive global climate shock $g > 0$. In addition, the effect is stronger with a higher b*

Proof. Note that $\lambda^s_{r_x - r_b} < 0$ and $\lambda_s^g > 0$ when $b > 1$. In addition, λ_s^g is increasing with country exposure b. □